Patterns formation in hyperbolic reaction–diffusion models with cross–diffusion

C. Currò[1], G. Valenti [2]
[1] MIFT, University of Messina,
Viale F. Stagno D'Alcontres 31, 98166, Messina, Italy
[2] Department of Engineering, University of Messina,
C.da di Dio, 98166, Messina, Italy
E-mail addresses: ccurro@unime.it, gvalenti@unime.it

Abstract

A class of hyperbolic reaction–diffusion models with cross-diffusion is derived within the context of Extended Thermodynamics.

Linear stability analysis is performed to study the nature of the equilibrium states against uniform and nonuniform perturbations. Emphasis is given to the occurrence of Hopf, Turing and Wave bifurcations. The weakly nonlinear analysis is then employed to deduce the equation governing the time evolution of pattern amplitude and to obtain the analytical approximated solution. The influence of the hyperbolic structure of the model on the pattern formation as well as on the transient regimes is highlighted. The theoretical predictions are illustrated on the hyperbolic Schnakenberg model and linear and weakly nonlinear stability are investigated both analytically and numerically.

Keywords: Hyperbolic model; Extended Thermodynamics; Pattern formation; Weakly nonlinear analysis.

MSC2010: 35B36, 35L40, 35Q92

1 Introduction

The study of pattern formation in biology, chemistry and physics is still nowadays a topic of great interest [1]–[6]. The occurrence of patterns in population

dynamics is usally investigated by means of reaction–diffusion models which consider the diffusion of each species depends only on the gradients of the concentration of the species itself. On the other hand, when the population pressures, due to the mutual interference between the individuals, affects the movements of competing species, one must take into account also the cross diffusion terms. Recently considerable attention has been devoted to the investigation of the stability behaviour of a system of interacting populations by taking into account the effects of self as well as cross-diffusion [7]–[18]. An appropriate description of biological phenomena which occur at macroscopic level is based upon continuum theory and the corresponding mathematical models usually take the form of parabolic reaction–diffusion equations [19]. However, the parabolic character of these models would lead the disease to propagate instantaneously over large distances. These unphysical features can be overcome by building up hyperbolic systems whose derivation are carried out by means of different mathematical approaches [3], [20]–[36]. We would like to stress that hyperbolicity guarantees finite speeds of propagation as it is expected in wave processes. Therefore, a more accurate description of transient phenomena, characterized by waves evolving in space over a finite time, should be performed via hyperbolic models.

In this paper we make use of the theoretical framework of the Extended Thermodynamics (ET) [37] to develop a general class of hyperbolic reaction-diffusion systems modelling those biological phenomena involving both self and cross-diffusion for two interacting species. We choose the ET approach in order to obtain a symmetric hyperbolic mathematical model which is satisfactory both on physical and mathematical points of view. In detail hyperbolicity guarantees realistic finite speed of propagation whereas the symmetric structure ensures mathematical properties, namely the well-posedness of Cauchy problems. Our goal is to elucidate how hyperbolicity affects the pattern formation as well as the transient dynamics from an homogeneous steady state to a patterned one. In particular, we point out the occurrence of wave instability in our hyperbolic model for two interacting species whereas, as well known, in the parabolic case one needs at least three reaction-diffusion equations [38]–[40].

The paper is organized as follows. In Section 2, along the leading ideas of ET, we build up the general class of hyperbolic reaction–diffusion models for two species which are subject to both self and cross-diffusion. In Section 3, we perform a linear stability analysis on the steady states with respect to both homogeneous and non-homogeneous perturbations focusing on the

occurrence of Hopf, Turing and Wave bifurcation. In Section 4, through a weakly nonlinear multiple scale analysis, we derive the Stuart–Landau equation ruling the evolution of the pattern amplitude in the supercritical case. In Section 5 we apply our general analysis to the one-dimensional Schnakenberg model and we investigate, both analytically and numerically, linear and weakly nonlinear stability. Finally, concluding remarks are addressed in the last Section.

2 Hyperbolic reaction–diffusion models with cross–diffusion

Reaction–diffusion models which take into account the effects of self as well cross–diffusion are widely used to describe spatio–temporal dynamics of two interacting species [7], [19]. The mathematical structure of these models, in one dimensional space and adimensional vector form, reads

$$\mathbf{W}_t = \mathbf{D}\mathbf{W}_{xx} + \mathbf{F}(\mathbf{W}) \tag{1}$$

where x and t are the space and time coordinates, respectively , and, hereafter, a subscript denotes the derivative with respect to the indicated variable. In (1) $\mathbf{W} \in R^2$ is a column vector denoting the field variables, $\mathbf{D}$ is the non–diagonal diffusion matrix and $\mathbf{F}(\mathbf{W})$ takes into account the reactive mechanisms. More precisely we have

$$\mathbf{W} = \begin{bmatrix} u \\ v \end{bmatrix}, \quad \mathbf{D} = \begin{bmatrix} 1 & d^v \\ d^u & d \end{bmatrix}, \quad \mathbf{F} = \gamma \begin{bmatrix} f(u,v) \\ g(u,v) \end{bmatrix} \tag{2}$$

with $d = \frac{D^v}{D^u}$, $d^u = \frac{D^{uv}}{D^u}$ and $d^v = \frac{D^{vu}}{D^u}$, being D^u, D^v , D^{uv} and D^{vu} the constant self–diffusion and cross–diffusion coefficients, respectively. In particular the self–diffusion coefficients are always positive whereas the cross–diffusion ones can be positive or negative. From a biological point of view the cross diffusion coefficient D^{vu} indicate the influence of v density to u density so if it is positive then u is repelled from v whereas if it is negative then u is attracted to v. D^{uv} has the same meaning with the role of u and v switched.

In (2) $f(u,v)$ and $g(u,v)$ represent the reaction kinetics whereas the parameter γ regulates the relative strength of the kinetic terms, or, alternatively, it gives the size of the spatial domain and the time scale, i.e. $\sqrt{\gamma}$ is

proportional to the linear dimension of the domain. The initial conditions must be described through non-negative bounded functions.

In system (1) diffusion mechanisms occur through Fick's law, namely the diffusion fluxes $\mathbf{J} \in R^2$ are assumed to be proportional to the gradient of the densities

$$\mathbf{J} = \begin{bmatrix} J^u \\ J^v \end{bmatrix} = -\mathbf{D}\mathbf{W}_x. \tag{3}$$

However Fickian diffusion unrealistically implies an infinite speed in the sense that any localized density disturbance instantaneously propagates to every part of the system. This unphysical feature can be avoided by making use of hyperbolic models and this goal may be achieved by means of different mathematical approaches, see [25], [33] and references therein quoted. Therefore, in this section, we develope an hyperbolic reaction–diffusion model by following the guidelines of the Extended Thermodynamic theory [37]. First of all, we assume the diffusion fluxes $\mathbf{J}$ as additional field variables satisfying the following balance equations

$$\mathbf{J}_t + \mathbf{T}_x = \mathbf{G} \tag{4}$$

where the constitutive functions $\mathbf{T}$ and $\mathbf{G}$ must be determined in terms of the whole set of the independent variables (u, v, J^u, J^v). At this step the system is not close because the constitutive functions $\mathbf{T}$ and $\mathbf{G}$ occurring in (4) are not known and it is the task of the constitutive theory established in ET to determine those functions or, at least, to reduce their generality. Therefore, since we are interested in a process not far away from the thermodynamical equilibrium characterized by vanishing $\mathbf{J}$, firstly we suppose a linear dependence of $\mathbf{T}$ and $\mathbf{G}$ on the fluxes namely

$$\begin{aligned} \mathbf{T} &= \begin{bmatrix} \mu\,(u,v) + \mu_1(u,v)J^u + \mu_2(u,v)J^v \\ \nu\,(u,v) + \nu_1(u,v)J^u + \nu_2(u,v)J^v \end{bmatrix}, \\ \mathbf{G} &= \begin{bmatrix} \rho\,(u,v) + \rho_1(u,v)J^u + \rho_2(u,v)J^v \\ \delta\,(u,v) + \delta_1(u,v)J^u + \delta_2(u,v)J^v \end{bmatrix}. \end{aligned} \tag{5}$$

Then, after inserting (5) into (4), we require that the resulting evolution equations reduce to Fick's law (3) in the stationary case so that the constitutive relations (5) become

$$\mathbf{T} = \begin{bmatrix} \mu\,(u,v) \\ \nu\,(u,v) \end{bmatrix} \qquad \mathbf{G} = \begin{bmatrix} -\mu_u J^u \\ -\frac{\nu_v}{d} J^v \end{bmatrix} \tag{6}$$

with

$$\begin{aligned} \mu_v - d^v\,\mu_u = 0 \quad &\Rightarrow \quad \mu(u,v) = \mu\,(u + d^v v) \\ d\,\nu_u - d^u\,\nu_v = 0 \quad &\Rightarrow \quad \nu(u,v) = \nu\,(d^u u + d\,v)\,. \end{aligned} \tag{7}$$

Therefore, the parabolic reaction–diffusion model (1) is replaced by

$$\mathbf{U}_t + \mathbf{M}(\mathbf{U})\mathbf{U}_x = \mathbf{B}(\mathbf{U}) \tag{8}$$

being

$$\mathbf{U} = \begin{bmatrix} u \\ v \\ J^u \\ J^v \end{bmatrix}, \quad \mathbf{M} = \begin{bmatrix} 0 & 0 & 1 & 0 \\ 0 & 0 & 0 & 1 \\ \mu_u & \mu_v & 0 & 0 \\ \nu_u & \nu_v & 0 & 0 \end{bmatrix}, \quad \mathbf{B} = \begin{bmatrix} \gamma f(u,v) \\ \gamma\, g(u,v) \\ -\mu_u\, J^u \\ -\frac{\nu_v}{d} J^v \end{bmatrix}. \tag{9}$$

A further restriction on the constitutive functions (7) arises from the entropy principle which assumes the existence of a concave entropy density η and an entropy flux ϕ satisfying the well-known entropy inequality

$$\eta_t + \phi_x = \Sigma \geq 0 \tag{10}$$

for all solutions of system (8). Here $\eta = \eta(u, v, J^u, J^v)$, $\phi = \phi(u, v, J^u, J^v)$ and the entropy production $\Sigma = \Sigma(u, v, J^u, J^v)$ are constitutive quantities.

Compatibility of system (8) with entropy inequality (10) can be achieved through the so-called Lagrange multipliers [37], [41] Λ, Γ, Π, Ω, depending on the whole set of the field variables. Indeed, the inequality

$$\begin{aligned} &\eta_t + \phi_x - \Lambda\,(u_t + J^u_x - \gamma f) - \Gamma\,(v_t + J^v_x - \gamma g) - \\ &-\Pi\,(J^u_t + \mu_u u_x + \mu_u d^v v_x + \mu_u J^u) - \Omega\left(J^v_t + \nu_v \tfrac{d^u}{d} u_x + \nu_v v_x + \tfrac{\nu_v}{d} J^v\right) \geq 0 \end{aligned} \tag{11}$$

must hold for arbitrary derivatives (u_t, v_t, J^u_t, J^v_t, u_x, v_x, J^u_x, J^v_x) so that it implies

$$\begin{aligned} &\mathrm{d}\,\eta = \Lambda\,\mathrm{d}\,u + \Gamma\,\mathrm{d}\,v + \Pi\,\mathrm{d}\,J^u + \Omega\,\mathrm{d}\,J^v \\ &\mathrm{d}\,\phi = \Lambda\,\mathrm{d}\,J^u + \Gamma\,\mathrm{d}\,J^v + \left(\Pi\mu_u + \Omega\nu_v \tfrac{d^u}{d}\right)\mathrm{d}\,u + \left(\Pi\mu_u d^v + \Omega\nu_v\right)\mathrm{d}\,v \\ &\Sigma = \Lambda\gamma f + \Gamma\gamma g - \Pi\mu_u J^u - \Omega\tfrac{\nu_v}{d} J^v \geq 0. \end{aligned} \tag{12}$$

From(12) we have

$$\begin{aligned}
&\Lambda = \Lambda_0(u,v) + \tfrac{\pi_{1u}}{2} J^u J^u + \pi_{2u} J^u J^v + \tfrac{\Omega_{2u}}{2} J^v J^v,\\
&\Gamma = \Gamma_0(u,v) + \tfrac{\pi_{1v}}{2} J^u J^u + \pi_{2v} J^u J^v + \tfrac{\Omega_{2v}}{2} J^v J^v,\\
&\Pi = \pi_1(u,v) J^u + \pi_2(u,v) J^v,\\
&\Omega = \pi_2(u,v) J^u + \Omega_2(u,v) J^v,
\end{aligned} \tag{13}$$

where

$$\pi_1(u,v) = \tfrac{d\Lambda_{0u} - d^u\Lambda_{0v}}{\mu_u(d-d^u d^v)}, \qquad \pi_2(u,v) = \tfrac{d(\Lambda_{0v} - d^v\Lambda_{0u})}{\nu_v(d-d^u d^v)}, \quad \Omega_2(u,v) = \tfrac{d(\Gamma_{0v} - d^v\Lambda_{0v})}{\nu_v(d-d^u d^v)},$$
$$\Lambda_{0v} = \Gamma_{0u}, \qquad (\nu_v - \mu_u)\Lambda_{0v} + d^v\mu_u\Lambda_{0u} - \tfrac{d^u}{d}\nu_v\Gamma_{0v} = 0.$$

Furthermore, taking into account $(12)_{1,2}$, the entropy density and the entropy flux assume the following form

$$\begin{aligned}
&\eta = \eta_0(u,v) + \frac{\pi_1}{2} J^u J^u + \pi_2 J^u J^v + \frac{\Omega_2}{2} J^v J^v,\\
&\phi = \Lambda_0(u,v) J^u + \Gamma_0(u,v) J^v,
\end{aligned} \tag{14}$$

with

$$\tfrac{\partial\eta_0}{\partial u} = \Lambda_0, \qquad \tfrac{\partial\eta_0}{\partial v} = \Gamma_0. \tag{15}$$

Finally, the concavity condition for η with respect to the field variables yields the further restrictions

$$\begin{aligned}
&d\Lambda_{0u} - d^u\Lambda_{0v} < 0, \qquad \Gamma_{0v} - d^v\Lambda_{0v} < 0, \qquad \Lambda_{0u} < 0, \qquad \Gamma_{0v} < 0,\\
&\Lambda_{0u}\Gamma_{0v} - \Lambda_{0v}^2 > 0, \qquad d - d^u d^v > 0, \qquad \mu_u > 0, \qquad \nu_v > 0,
\end{aligned} \tag{16}$$

which provide the positiveness of the relaxation times $\tau^u = \dfrac{1}{\mu_u}$ and $\tau^v = \dfrac{d}{\nu_v}$, as expected. We remark that the concavity condition for η with respect to the field variables guarantees the governing system (8) to be symmetric–hyperbolic in the sense of Friedrichs–Lax [42] when the Lagrange multipliers are chosen as field variables. The advantage of having symmetric hyperbolic systems lies in the fact that there exist theorems guaranteeing the well-posedness for the Cauchy problem , i.e. existence, uniqueness, and continuous dependence of the solutions on the data [37], [43].

In passing we notice that in the limit case $\tau^u \to 0$ and $\tau^v \to 0$ the hyperbolic model (8) reduces to the corresponding parabolic one (1).

Finally, as it is easy to ascertain, the four real characteristic velocities λ associated to the system (8) are obtained from

$$\lambda^2 = \frac{1}{2}\left(\mu_u + \nu_v \pm \sqrt{(\mu_u - \nu_v)^2 + 4\frac{d^u d^v}{d}\mu_u \nu_v}\right). \tag{17}$$

3 Linear stability analysis

Le us suppose that the system (8) admits the steady state $\mathbf{U}^* = (u^*, v^*, 0, 0)$, which is solution of $\mathbf{B}(\mathbf{U}) = 0$, with $u^* > 0$, $v^* > 0$.

In order to investigate the stability character of this steady state, we linearize Eqs.(8) around $\mathbf{U}^*$ by looking for solutions of the form

$$\mathbf{U} = \mathbf{U}^* + \overline{\mathbf{U}} \exp\left(\omega t + \mathrm{i}\, k\, x\right) \tag{18}$$

where ω and k are the growth factor and the real wave number, respectively. Consequently we obtain

$$\left(\omega \mathbf{I} + \mathrm{i}\, k \mathbf{M}^* - (\nabla \mathbf{B})^*\right) \overline{\mathbf{U}} = \mathbf{0} \tag{19}$$

where $\mathbf{I}$ is the 4×4 identity matrix, the asterisk denotes the evaluation of the quantities at $\mathbf{U}^*$ and $\nabla \equiv \dfrac{\partial}{\partial \mathbf{U}}$. Then, the system (19) admits non–trivial solutions iff the following characteristic equation holds

$$\omega^4 + A_1\omega^3 + A_2\omega^2 + A_3\omega + A_4 = 0 \tag{20}$$

with

$$\begin{aligned}
A_1 &= \mu_u^* + \frac{\nu_v^*}{d} - \gamma\left(f_u^* + g_v^*\right), \\
A_2 &= \left(\mu_u^* + \nu_v^*\right) k^2 + b_2, \\
A_3 &= a_3 k^2 + b_3, \\
A_4 &= \frac{\mu_u^* \nu_v^*}{d}\left[\left(d - d^u d^v\right) k^4 + a_4 k^2 + b_4\right],
\end{aligned} \tag{21}$$

being

$$
\begin{aligned}
b_2 &= \frac{\mu_u^*\nu_v^*}{d} - \gamma\left(f_u^* + g_v^*\right)\left(\mu_u^* + \frac{\nu_v^*}{d}\right) + \gamma^2\left(f_u^* g_v^* - f_v^* g_u^*\right), \\
a_3 &= (d+1)\,\frac{\mu_u^*\nu_v^*}{d} + \gamma\left(d^v g_u^* - g_v^*\right)\mu_u^* + \gamma\left(\frac{d^u}{d} f_v^* - f_u^*\right)\nu_v^*, \\
b_3 &= \gamma^2\left(f_u^* g_v^* - f_v^* g_u^*\right)\left(\mu_u^* + \frac{\nu_v^*}{d}\right) - \gamma\left(f_u^* + g_v^*\right)\frac{\mu_u^*\nu_v^*}{d}, \\
a_4 &= -\gamma\left(d f_u^* + g_v^* - d^v g_u^* - d^u f_v^*\right), \\
b_4 &= \gamma^2\left(f_u^* g_v^* - f_v^* g_u^*\right).
\end{aligned}
$$

As is well known if the real part of all roots of equation (20) are negative $\forall k$ then $\mathbf{U}^*$ is linearly stable. Therefore the stability of the equilibrium state can be discussed by using the Routh-Hurwitz criterion, i.e.

$$
\mathrm{Re}\,\omega < 0 \quad \forall\,\omega \Leftrightarrow A_1 > 0,\ A_3 > 0,\ A_4 > 0,\ A_1 A_2 A_3 > A_3^2 + A_1^2 A_4\ \forall k. \tag{22}
$$

It is straightforward to ascertain that, in the absence of diffusion, namely for spatially homogeneous perturbations ($k = 0$), the equation (20) can be factorized as

$$
\left(\omega^2 + (\mu_u^* + \frac{\nu_v^*}{d})\omega + \frac{\mu_u^*\nu_v^*}{d}\right)\left(\omega^2 - \gamma(f_u^* + g_v^*)\omega + \gamma^2\left(f_u^* g_v^* - f_v^* g_u^*\right)\right) \tag{23}
$$

whose roots are given by

$$
\begin{aligned}
\omega_1 &= -\frac{\nu_v^*}{d}, \\
\omega_2 &= -\mu_u^*, \\
\omega_{3,4} &= \frac{\gamma}{2}\left(\left(f_u^* + g_v^*\right) \pm \sqrt{\left(f_u^* + g_v^*\right)^2 - 4\left(f_u^* g_v^* - f_v^* g_u^*\right)}\right)
\end{aligned} \tag{24}
$$

so that, being $\omega_{1,2}$ always real and negative, the steady state $\mathbf{U}^*$ is asymptotically linearly stable iff

$$
f_u^* + g_v^* < 0, \qquad f_u^* g_v^* - f_v^* g_u^* > 0. \tag{25}
$$

Therefore, under assumptions (25), A_1 and A_2 are positive for all k and, in turn, the condition $A_3 > 0$ is redundant. Consequently, the Routh-Hurwitz criterion requires

$$
\mathrm{Re}\,\omega < 0 \quad \forall\,\omega \ \Leftrightarrow\ A_4 > 0, \qquad A_1 A_2 A_3 - A_3^2 - A_1^2 A_4 > 0 \qquad \forall k. \tag{26}
$$

For further convenience, in order to investigate the Routh-Hurwitz conditions (26), we introduce the following polynomials of degree two in k^2

$$\begin{aligned}\Xi_1(k^2) &= \frac{d}{\mu_u^*\nu_v^*}A_4 = (d - d^u d^v)k^4 + a_4 k^2 + b_4 \\ \Xi_2(k^2) &= A_1 A_2 A_3 - A_3^2 - A_4 A_1^2 = \xi_2\, k^4 + \xi_1\, k^2 + \xi_0\end{aligned} \tag{27}$$

where

$$\begin{aligned}\xi_0 &= A_1 b_2 b_3 - b_3^2 - \frac{\mu_u^*\nu_v^*}{d}A_1^2 b_4, \\ \xi_1 &= (\mu_u^* + \nu_v^*)A_1 b_3 + A_1 b_2 a_3 - 2a_3 b_3 - \frac{\mu_u^*\nu_v^*}{d}A_1^2 a_4, \\ \xi_2 &= (\mu_u^* + \nu_v^*)A_1 a_3 - a_3^2 - \frac{\mu_u^*\nu_v^*}{d}(d - d^u d^v)A_1^2.\end{aligned} \tag{28}$$

Therefore this linear stability analysis reveals two main types of instability associated to homogeneous ($k = 0$) or nonhomogeneous perturbations ($k \neq 0$) related to Hopf and diffusion–driven instability, respectively.

First of all we look for the occurrence of a space independent Hopf bifurcation which breaks the temporal symmetry of the system, namely gives rise to oscillations which are uniform in space and periodic in time.

Proposition 1 *Space-independent Hopf bifurcation*

Let p_{cr} the critical value of a control parameter p then the model (8) undergoes a space-independent Hopf bifurcation around the equilibrium $\mathbf{U}^*$ iff the following conditions are satisfied

$$f_u^* + g_v^*|_{p_{cr}} = 0, \qquad f_u^* g_v^* - f_v^* g_u^*|_{p_{cr}} > 0, \qquad \frac{\mathrm{d}}{\mathrm{d}\,p}\,(f_u^* + g_v^*)\bigg|_{p_{cr}} \neq 0. \tag{29}$$

`Proof` As known, a space-independent Hopf bifurcation occurs when the characteristic equation (20) evaluated at $k = 0$ admits a pair of purely imaginary roots and no other roots with null real part together with the transversality condition $\frac{\mathrm{d}\,\mathrm{Re}(\omega)}{\mathrm{d}\,p}\Big|_{p_{\mathrm{cr}}} \neq 0$.

In detail, from (24) it follows that $\omega_{1,2}$ are always negative and $\mathrm{Re}(\omega_{3,4}) = 0$ iff $(29)_{1,2}$ hold whereas the trasversality condition becomes

$$\frac{\mathrm{d}\,\mathrm{Re}\,(\omega)}{\mathrm{d}\,p}\bigg|_{p_{\mathrm{cr}}} = \frac{\gamma}{2}\,\frac{\mathrm{d}}{\mathrm{d}\,p}\,(f_u^* + g_v^*)\bigg|_{p_{\mathrm{cr}}} \neq 0. \tag{30}$$

Therefore $(29)_1$ represents the Hopf bifurcation line and in turn $\mathbf{U}^*$ becomes unstable as $f_u^* + g_v^* > 0$.

Now we consider diffusion–driven instabilities occurring when the homogeneous steady state, linearly stable in the absence of diffusion, becomes unstable when diffusion is present. Mathematically speaking, the occurrence of diffusion–driven instability requires the existence of some $k \neq 0$ such that $\mathrm{Re}(\omega) > 0$ whereas $\mathrm{Re}(\omega) < 0$ for $k = 0$.

Proposition 2 *Diffusion-driven instabilities*

Let us assume the equilibrium point $\mathbf{U}^*$ *stable with respect to uniform perturbations, namely*

$$f_u^* + g_v^* < 0, \qquad f_u^* g_v^* - f_v^* g_u^* > 0 \tag{31}$$

then the model (8) exhibits diffusion–driven instability around $\mathbf{U}^*$ *iff at least one of the following conditions is satisfied*

(i)

$$a_4 + 2\sqrt{(d - d^u d^v) b_4} < 0 \tag{32}$$

(ii)

$$\xi_2 < 0 \quad or \quad \begin{cases} \xi_2 > 0 \\ \xi_1 + 2\sqrt{\xi_0 \xi_2} < 0 \end{cases} \tag{33}$$

`Proof` Bearing in mind the analysis carried on hitherto, the occurrence of diffusion–driven instability is observed iff at least one of the two inequalities in (26) is violated. This goal can be achieved by checking the sign of Ξ_1 and Ξ_2 defined in (27).

First of all we focus our attention on $\Xi_1(k^2)$ which, being $d - d^u d^v > 0$ and, owing to $(31_2$, $b_4 > 0$, changes its sign if and only if

$$a_4 < 0, \qquad a_4^2 - 4(d - d^u d^v) b_4 > 0$$

and in turn

$$\Xi_1(k^2) > 0 \quad \forall\, k \Leftrightarrow a_4 + 2\sqrt{(d - d^u d^v) b_4} > 0. \tag{34}$$

For what concerns the sign of $\Xi_2(k^2)$, firstly we observe that, under the assumptions (31), ξ_0 is always positive

$$\begin{aligned}
&\xi_0 = -\gamma \left(\mu_u^* + \tfrac{\nu_v^*}{d}\right)(f_u^* + g_v^*) \\
&\left\{\gamma^4 (f_u^* g_v^* - f_v^* g_u^*)^2 - \gamma^3 \left(\mu_u^* + \tfrac{\nu_v^*}{d}\right)(f_u^* + g_v^*)(f_u^* g_v^* - f_v^* g_u^*) + \right. \\
&+\gamma^2 \left(\mu_u^{*\,2} + \tfrac{\nu_v^{*\,2}}{d^2}\right)(f_u^* g_v^* - f_v^* g_u^*) + \gamma^2 \tfrac{\mu_u^* \nu_v^*}{d}(f_u^* + g_v^*)^2 - \\
&\left. -\gamma \tfrac{\mu_u^* \nu_v^*}{d}(f_u^* + g_v^*)\left(\mu_u^* + \tfrac{\nu_v^*}{d}\right) + \left(\tfrac{\mu_u^* \nu_v^*}{d}\right)^2 \right\} > 0.
\end{aligned} \tag{35}$$

Consequently, being $\Xi_2(k^2)$ a quadratic polynomial in k^2 such that $\Xi_2(0) = \xi_0 > 0$, the shape of $\Xi_2(k^2)$ depends on the sign of the leading coefficient ξ_2. More precisely we have

$$\begin{aligned}
&\xi_2 > 0 \;\Rightarrow\; \Xi_2(k^2) > 0 \quad \forall\, k \;\Leftrightarrow\; \xi_1 > 0 \quad \text{or} \quad \xi_1^2 - 4\xi_0\xi_2 < 0 \\
&\xi_2 < 0 \;\Rightarrow\; \exists\, \overline{k}^2 \;:\quad \Xi_2(k^2) \le 0 \quad \text{for} \quad k^2 \ge \overline{k}^2
\end{aligned} \tag{36}$$

and in turn

$$\Xi_2(k^2) > 0 \quad \forall\, k \;\Leftrightarrow\; \begin{cases} \xi_2 > 0 \\ \xi_1 + 2\sqrt{\xi_0 \xi_2} > 0. \end{cases} \tag{37}$$

In passing we notice that the sign of both ξ_1 and ξ_2 depends on the model parameters as well as on the constitutive ones μ_u^* and ν_v^*.

Therefore, violation of $(26)_1$ corresponds to condition (32) whereas violation of $(26)_2$ leads to (33).

Remark. The proposition 2 points out two different ways to destabilize, via diffusion, the homogeneous steady state $\mathbf{U}^*$ related to the Turing and wave instability, respectively [1]. In particular, the Turing bifurcation corresponds to $\mathrm{Re}(\omega) = \mathrm{Im}(\omega) = 0$ at $k = k_c \neq 0$ occurring when $\Xi_1(k^2) = 0$ while the wave bifurcation occurs when $\mathrm{Re}(\omega) = 0$, $\mathrm{Im}(\omega) \neq 0$ at $k = k_w \neq 0$ i.e. for $\Xi_2(k^2) = 0$.

In fact, by requiring $\omega(k^2) = \mathrm{i}\,\theta$, from (20) the following conditions are easily obtained

$$\begin{cases} \theta(A_3 - \theta^2 A_1) = 0 \\ \theta^4 - A_2\theta^2 + A_4 = 0 \end{cases} \Rightarrow \begin{array}{l} \omega(k^2) = \Xi_1(k^2) = 0 \\ \text{or} \\ \omega(k^2) = \pm\,\mathrm{i}\sqrt{\frac{A_3}{A_1}},\ \Xi_2(k^2) = 0. \end{array}$$

Consequently, a change in the sign of Ξ_1 or Ξ_2 can produce spatial or spatio–temporal patterns, respectively. Therefore, under assumption (25), except for degenerate situations, Proposition 2 predicts two qualitatively different ways to get diffusion–driven instabilities.

Turing instability

We choice the set of parameters such that

$$\begin{cases} \Xi_1(k^2) < 0 \\ \Xi_2(k^2) > 0 \end{cases} \Leftrightarrow \begin{cases} a_4 + 2\sqrt{(d - d^u d^v) b_4} < 0 \\ \xi_2 > 0 \\ \xi_1 + 2\sqrt{\xi_0 \xi_2} > 0 \end{cases}$$

then the spatially homogeneous steady state $\mathbf{U}^*$ becomes linearly unstable to perturbations with wave numbers k such that $k^2 \in (k_1^2, k_2^2)$, being k_1^2 and k_2^2 roots of the equation $\Xi_1(k^2) = 0$, namely

$$k_{1,2}^2 = \frac{-a_4 \mp \sqrt{a_4^2 - 4(d - d^u d^v) b_4}}{2(d - d^u d^v)}. \tag{38}$$

Furthermore, the onset of diffusion–driven instability, corresponding to $\omega = 0$ and $\frac{\mathrm{d}\omega}{\mathrm{d}k} = 0$, determines the critical values of the control parameter d_c and of the wave number k_c, namely

$$\begin{aligned} d_c &= \frac{f_u^* g_v^* - 2 f_v^* g_u^* + f_u^* (d^u f_v^* + d^v g_u^*) + 2\sqrt{(f_u^* g_v^* - f_v^* g_u^*)(d^v f_u^* - f_v^*)(g_u^* - d^u f_u^*)}}{f_u^{*2}} \\ k_c^2 &= \gamma \sqrt{\frac{f_u^* g_v^* - f_v^* g_u^*}{d_c - d^u d^v}}. \end{aligned} \tag{39}$$

Therefore when the diffusion coefficient ratio d increases beyond d_c, spatial patterns arise.

Finally, by considering the further restriction on the diffusion coefficients imposed by the reality of the critical parameter d_c, the full set of conditions

for Turing instability of system (8) becomes

$$\begin{aligned}
&d^u d^v < d,\\
&f_u^* + g_v^* < 0, \quad f_u^* g_v^* - f_v^* g_u^* > 0,\\
&df_u^* + g_v^* - d^v g_u^* - d^u f_v^* > 0,\\
&\left(df_u^* + g_v^* - d^v g_u^* - d^u f_v^*\right)^2 - 4\left(d - d^u d^v\right)\left(f_u^* g_v^* - f_v^* g_u^*\right) > 0,\\
&\left(d^v f_u^* - f_v^*\right)\left(g_u^* - d^u f_u^*\right) > 0,\\
&\xi_2 > 0, \quad \xi_1 + 2\sqrt{\xi_0 \xi_2} > 0.
\end{aligned} \tag{40}$$

Summarizing, from (38) and (39) it is easy to see that the hyperbolicity of the system has no effect on the unstable modes having k_1^2, k_2^2, d_c and k_c exactly the same expressions as for the standard reaction–diffusion model. Neverthless, owing to $(40)_6$, the hyperbolic character of the governing model modifies the Turing regions through the constitutive parameters μ_u^*, ν_v^*. Unfortunately the conditions $(40)_6$ cannot be easily managed so that significant information could be extracted through numerical investigations.

Wave instability

Unlike to parabolic two species reaction–diffusion systems, the homogeneous steady state $\mathbf{U}^*$ can undergo a wave instability if the conditions (31) are satisfied and

$$\begin{cases} a_4 + 2\sqrt{(d - d_u d_v) b_4} > 0 \\ \xi_2 < 0 \end{cases} \quad or \quad \begin{cases} a_4 + 2\sqrt{(d - d_u d_v) b_4} > 0 \\ \xi_2 > 0 \\ \xi_1 + 2\sqrt{\xi_0 \xi_2} < 0 \end{cases} \tag{41}$$

so that spatio–temporal patterns may arise. This type of instabilities typically occurs in parabolic reaction–diffusion models involving at least three species [38]–[40] whereas it has been investigated for special hyperbolic reaction diffusion equations involving only two species [21], [23], [44].

In particular, taking into account $(36)_2$, the choice of the set parameters satisfying $(41)_1$ leads to many unstable modes corresponding to wave numbers $k^2 > \overline{k}^2$. In this case, as already evidentiated for the random walk Turing model [21], the wave character prevails with respect to the diffusive one and a nonlinear analysis should be necessary in order to understand the dominating modes and the stable oscillating states.

On the other hand, if the conditions $(33)_2$ hold then equation $\Xi_2(k^2) = 0$ admits two real positive roots

$$k_{1,2}^2 = \frac{-\xi_1 \pm \sqrt{\xi_1^2 - 4\xi_0\xi_2}}{2\xi_2} \tag{42}$$

and the model undergoes a wave instability when

$$\xi_1^2 - 4\xi_0\xi_2 = 0 \tag{43}$$

which defines the critical value of the control parameter d_w and, in turn, the critical wave number k_w is obtained, namely

$$k_w^2 = -\frac{\xi_1}{2\xi_2}. \tag{44}$$

As it is straightforward to ascertain, both d_w and k_w depend on the constitutive parameters μ_u^*, ν_v^* and the wave instability cannot occur for small relaxation times τ^u, τ^v, i.e. in the parabolic limit where $\xi_1 > 0$.

Unfortunately it is rather cumbersome to derive the explicit analytical expressions for d_w and k_w so that a further numerical investigation will be required. Neverthless, in this paper we are mainly concerned with Turing instability whereas further investigation of wave instabilities will be the subject of a future work.

4 Weakly nonlinear analysis

The linear stability analysis carried on in the previous section, is only valid for small time and infinitesimal perturbations. For long time, the growth of the unstable modes is dominated by the nonlinear terms whose influence on the spatial patterns can be investigated by using a standard perturbative approach [1], [11], [12], [45]. Therefore, under the assumption of constant constitutive parameters μ_u^* and ν_v^*, we make use of a weakly nonlinear analysis to describe the dynamics close to the critical bifurcation parameter d_c. To this aim we expand the field variables $\mathbf{U}$ as well as the parameter d and we introduce a hierarchy of time scales as follows

$$\begin{aligned}
&\mathbf{U} = \mathbf{U}^* + \varepsilon\mathbf{U}_1 + \varepsilon^2\mathbf{U}_2 + \varepsilon^3\mathbf{U}_3 + \mathcal{O}\left(\varepsilon^4\right) \\
&d = d_c + \varepsilon d_1 + \varepsilon^2 d_2 + \varepsilon^3 d_3 + \mathcal{O}\left(\varepsilon^4\right) \\
&\frac{\partial}{\partial t} = \varepsilon\frac{\partial}{\partial T_1} + \varepsilon^2\frac{\partial}{\partial T_2} + \varepsilon^3\frac{\partial}{\partial T_3} + \mathcal{O}\left(\varepsilon^4\right)
\end{aligned} \tag{45}$$

where $\epsilon \ll 1$ is a positive small parameter. Substituting the above expansions into the governing system (8) and collecting terms of the same orders of ε we obtain the following set of linear equations

$$\begin{aligned} &\text{at order 1} \qquad \frac{\partial \mathbf{U}_1}{\partial x} - \mathbf{K}^* \mathbf{U}_1 = \mathbf{0} \\ &\text{at order 2} \qquad \frac{\partial \mathbf{U}_2}{\partial x} - \mathbf{K}^* \mathbf{U}_2 = \left(\mathbf{M}^{-1}\right)^* \mathbf{H} \\ &\text{at order 3} \qquad \frac{\partial \mathbf{U}_3}{\partial x} - \mathbf{K}^* \mathbf{U}_3 = \left(\mathbf{M}^{-1}\right)^* \mathbf{N} \end{aligned} \tag{46}$$

being

$$\mathbf{K}^* = \left(\mathbf{M}^{-1} \nabla \mathbf{B}\right)^* \tag{47}$$

whereas the explicit expressions of $\mathbf{H}$ and $\mathbf{N}$ are given in the Appendix. After inserting the above expansions into the governing system (8) and by requiring compatibility conditions, we obtain the searched solution. The detailed calculation, for the sake of simplicity, have been carried on in the Appendix and the following approximated solution, up to the second order, has been obtained

$$\mathbf{U} = \mathbf{U}^* + \varepsilon\, \mathcal{A} \begin{bmatrix} \mathbf{r}\, \cos\left(k_c\, x\right) \\ \widehat{\mathbf{r}}\, \sin\left(k_c\, x\right) \end{bmatrix} + \varepsilon^2\, \mathcal{A}^2 \begin{bmatrix} \mathbf{U}_{20} + \mathbf{U}_{22}\, \cos\left(2k_c\, x\right) \\ \widehat{\mathbf{U}}_{22}\, \sin\left(2k_c\, x\right) \end{bmatrix} + \mathcal{O}(\varepsilon^3) \tag{48}$$

with the expressions of the vectors $\mathbf{r}$, $\widehat{\mathbf{r}}$, $\mathbf{U}_{20}$, $\mathbf{U}_{22}$, $\widehat{\mathbf{U}}_{22}$ provided in the Appendix. The pattern amplitude $\mathcal{A}(T_2)$ satisfy the following Stuart–Landau equation

$$\frac{\mathrm{d}\,\mathcal{A}}{\mathrm{d}\,T_2} = \sigma \mathcal{A} - L\,\mathcal{A}^3. \tag{49}$$

where the growth rate σ and the Landau coefficient L are given by

$$\begin{aligned} \sigma &= \frac{d_2 k_c^2 \left(\gamma f_u^* - k_c^2\right)}{(1+d_c)k_c^2 - \gamma(f_u^* + g_v^*) + [\gamma k_c^2 (d_c f_u^* - d^u f_v^*) - \gamma^2 (f_u^* g_v^* - f_v^* g_u^*)]\left(\frac{d_c}{\nu_v^*} - \frac{1}{\mu_u^*}\right)} \\ L &= \frac{(p_1 + 8q_1 + 4s_1)\left(k_c^2 d^u - \gamma g_u^*\right) + (p_2 + 8q_2 + 4s_2)\left(\gamma f_u^* - k_c^2\right)}{8 r_2 \left\{(1+d_c)k_c^2 - \gamma(f_u^* + g_v^*) + [\gamma k_c^2 (d_c f_u^* - d^u f_v^*) - \gamma^2 (f_u^* g_v^* - f_v^* g_u^*)]\left(\frac{d_c}{\nu_v^*} - \frac{1}{\mu_u^*}\right)\right\}} \end{aligned} \tag{50}$$

with the coefficients $p_1, q_1, s_1, p_2, q_2, s_2$ provided in the Appendix. The equation (49), obtained by performing the weakly nonlinear analysis up to the third order, is the canonical form for a dynamical system exhibiting a pitchfork bifurcation. More precisely, the Stuart–Landau equation (49) implies

that the perturbation amplitude change depends on both linear and nonlinear contributions. Since σ is always positive in the pattern–forming region, the amplitude dynamics strongly depends on the sign of the nonlinear term that is on the sign of the Landau coefficient L. In particular, if $L < 0$ the perturbation grows infinitely so that the assumption of amplitude smallness breaks and higher order nonlinearities are necessary to obtain a stationary solution with a subcritical bifurcation. On the other hand, a positive Landau coefficient L, corresponding to a supercritical bifurcation, implies that the linear growth σ is balanced by the nonlinear term and the amplitude reachs a constant saturation value $\mathcal{A}_\infty = \sqrt{\frac{\sigma}{L}}$.

Hereafter we limit our analysis to the supercritical case, so that the asymptotic solution of the hyperbolic system (8) can be expressed as

$$\mathbf{U}_\infty = \mathbf{U}^* + \varepsilon \sqrt{\frac{\sigma}{L}} \begin{bmatrix} \mathbf{r} \cos(k_c\, x) \\ \widehat{\mathbf{r}} \sin(k_c\, x) \end{bmatrix} + \varepsilon^2 \frac{\sigma}{L} \begin{bmatrix} \mathbf{U}_{20} + \mathbf{U}_{22} \cos(2k_c\, x) \\ \widehat{\mathbf{U}}_{22} \sin(2k_c\, x) \end{bmatrix} + \mathcal{O}(\varepsilon^3). \tag{51}$$

As far as the equilibrium pattern is concerned, it should be observed that, as it is expected, $\mathcal{A}_\infty$ as well as $\mathbf{U}_\infty$ are not affected by the constitutive quantities μ_u^* and ν_v^*.

According to (48), the transitional regime from $\mathbf{U}^*$ to $\mathbf{U}_\infty$ is ruled by the evolution of the amplitude $\mathcal{A}(T_2)$ which, by integrating equation (49), reads

$$\mathcal{A}(T_2) = \frac{\mathcal{A}_\infty}{\sqrt{1 + \left(\frac{\mathcal{A}_\infty^2}{\mathcal{A}_{in}^2} - 1\right) \exp(-2\sigma\, T_2)}} \tag{52}$$

where $\mathcal{A}_{in} = \mathcal{A}(0)$ is the initial value of the amplitude $\mathcal{A}$. It follows that the $\mathcal{A}(T_2)$ depends on μ_u^* and ν_v^* through the growth factor σ except for a particular relation between the two constitutive parameters. Consequently the transient regime is affected by the relaxation times appearing in the parameter σ. More precisely, from $(50)_1$, we have

Proposition 3 *Let the Landau coefficient $L > 0$ and*

$$\nu_v^* = d_c \mu_u^* \tag{53}$$

then the transitional regime from the steady state $\mathbf{U}^*$ to the pattern equilibrium solution $\mathbf{U}_\infty$ is not affected by the constitutive parameters μ_u^*, ν_v^*.

Remark. The hyperbolic model exhibits the same transient dynamics of the parabolic one not only when the constitutive parameters are very large but also when they satisfy the relation (53). In fact, in both cases, taking into account the expression $(50)_1$, the growth rate σ and the Landau coefficient L approach to the corresponding values $\widehat{\sigma}$ and $\widehat{L}$ of the parabolic model

$$\widehat{\sigma} = \frac{d_2 k_c^2 \left(\gamma f_u^* - k_c^2\right)}{(1+d_c)k_c^2 - \gamma(f_u^* + g_v^*)}, \quad \widehat{L} = \frac{(p_1+8q_1+4s_1)\left(k_c^2 d^u - \gamma g_u^*\right) + (p_2+8q_2+4s_2)\left(\gamma f_u^* - k_c^2\right)}{8r_2[(1+d_c)k_c^2 - \gamma(f_u^* + g_v^*)]}. \tag{54}$$

On the contrary, for arbitrary values of the constitutive parameters, the transitional regime is ruled by the sign of the quantity

$$\Upsilon = \left[\gamma k_c^2 \left(d_c f_u^* - d^u f_v^*\right) - \gamma^2 \left(f_u^* g_v^* - f_v^* g_u^*\right)\right] \left(\frac{d_c}{\nu_v^*} - \frac{1}{\mu_u^*}\right) \tag{55}$$

involved in σ. More precisely, by denoting with $\widehat{\mathcal{A}}(T_2)$ the amplitude close to the parabolic limit, we have

$$\begin{aligned} &\Upsilon \geq 0 && \Rightarrow 0 < \sigma \leq \widehat{\sigma} \quad \Rightarrow \mathcal{A}(T_2) \leq \widehat{\mathcal{A}}(T_2) \\ &\gamma\left(f_u^* + g_v^*\right) - \left(1 + d_c\right) k_c^2 < \Upsilon < 0 && \Rightarrow \sigma > \widehat{\sigma} > 0 \quad \Rightarrow \mathcal{A}(T_2) > \widehat{\mathcal{A}}(T_2). \end{aligned} \tag{56}$$

In conclusion, from (56) it follows that, for fixed kinetic parameters, the difference between the relaxation times determines the behaviour of the transitional regime from $\mathbf{U}^*$ to the equilibrium pattern (51).

5 Schnakenberg model

In this section we apply the results previously obtained to Schnakenberg model describing an autocatalytic chemical reaction with possible oscillatory behavior. This model, recently investigated by several authors [13], [14], belongs to the general class of reaction–diffusion systems (1) where u is an activator, v a substrate and the kinetic terms are expressed as follows

$$\begin{aligned} f(u,v) &= a - u + u^2 v \\ g(u,v) &= b - u^2 v, \end{aligned} \tag{57}$$

being a and b non–dimensional positive parameters with $b > a$ such that the activator–depleted substrate model is obtained [46]–[48]. Hereafter we also

assume that the two chemical species u and v are repelled from each other so that the cross–diffusion coefficients d^u and d^v are both positive.

In line with the analysis developed in Section 2 the parabolic system is replaced by the hyperbolic one (8) which admits only unique positive steady state

$$\mathbf{U}^* = \left(\beta, \quad \frac{\beta+\alpha}{2\beta^2}, \quad 0, \quad 0 \right).$$

For simplicity of calculation, we have introduced the two new parameters

$$\beta = a + b, \qquad \alpha = b - a \tag{58}$$

so that for a fixed $\beta > 0$ it follows $\alpha \in (0, \beta)$.

It is easy to check that the linear stability character of $\mathbf{U}^*$ with respect to spatially homogeneous perturbations depends upon the value of the control parameters α and β. In fact, being

$$f_u^* = \frac{\alpha}{\beta}, \quad f_v^* = \beta^2, \quad g_u^* = -\frac{\alpha+\beta}{\beta}, \quad g_v^* = -\beta^2, \tag{59}$$

from (25) we have

$$\mathbf{U}^* \text{ stable for } \begin{cases} \beta \geqslant 1, \quad \alpha \in (0, \alpha_{\rm ex}), \\ \text{or} \\ \beta \in (0,1), \quad \alpha \in (0, \alpha_{\rm cr}) \end{cases} \tag{60}$$

being

$$\alpha_{\rm ex} = \beta, \qquad \alpha_{\rm cr} = \beta^3. \tag{61}$$

Therefore, if β is large then $\mathbf{U}^*$ is locally asymptotically stable with respect to homogeneous perturbations $\forall \alpha \in (0, \beta)$, whereas if $0 < \beta < 1$ the unique steady state is locally asymptotically stable for $0 < \alpha < \alpha_{\rm cr}$ and, according to Proposition 1, it loses its stability character at $\alpha = \alpha_{\rm cr}$ through a Hopf bifurcation. Indeed, when $\alpha = \alpha_{\rm cr}$, the characteristic equation (20) admits a pair of purely imaginary conjugate roots and the transversality condition

$$\left. \frac{\mathrm{d}\,\mathrm{Re}\,(\omega)}{\mathrm{d}\,\alpha} \right|_{\alpha_{\rm cr}} = \frac{\gamma}{2\beta} \neq 0 \tag{62}$$

is fulfilled.

It should be mentioned that recently the Hopf bifurcations of the reaction–diffusion Schanakenberg model without cross–diffusion has been investigated in [49], [50] and the uniqueness of the limit cycle of the corresponding ODE system has been proved in [51].

The investigation carried on in Section 3 allows us to obtain the necessary and sufficient conditions in order to the steady state $\mathbf{U}^*$ be asymptotically stable with respect to both homogeneous and non–homogeneous perturbations.

Proposition 4 *Let*

$$\alpha_T = \frac{\beta^3(1+d^u) - \beta d^v + 2\beta^2\sqrt{d - d^u d^v}}{d + d^v} \tag{63}$$

and the cross–diffusion parameters such that $d^u d^v \in (0, d)$*, then* $\mathbf{U}^*$ *is linear asymptotically stable with respect to small perturbations iff*

$$\xi_2 > 0, \quad \xi_1 + 2\sqrt{\xi_0 \xi_2} > 0, \tag{64}$$

and

$$\begin{cases} \beta \geqslant 1, \quad 0 < \alpha < \min\{\alpha_{ex}, \alpha_T\} \\ or \\ \beta \in (0,1), \quad 0 < \alpha < \min\{\alpha_{cr}, \alpha_T\} \end{cases} \tag{65}$$

with ξ_0, ξ_1, ξ_2 *given in (28).*

`Proof` According to the Routh–Hurwitz criterion (26), the steady state is linearly stable iff (60), (34) and (37) hold.

In particular the condition (34) reduces to

$$(d + d^v)\alpha - (1 + d^u)\beta^3 + d^v\beta - 2\beta^2\sqrt{d - d^u d^v} < 0 \tag{66}$$

which defines the upper threshold α_T for the control parameter α. Finally, by comparing (60) and (66), the condition (65) is obtained whereas the inequalities (64) coincide exactly with (37).

The value α_T is the threshold above which the steady state $\mathbf{U}^*$, stable with respect to small uniform perturbations, becomes unstable to the inhomogeneous ones owing to the presence of a null root of (20) which takes place at $\alpha = \alpha_T$ and gives rise to the onset of Turing diffusion–driven instability.

We remark that, once α, β are fixed according to (66), conditions (64) are trivially satisfied in the parabolic limit $\mu_u^* \gg 1$, $\nu_v^* \gg d$, otherwise they determine the allowed values for μ_u^*, ν_v^* in order to the present analysis hold.

Therefore, under the assumption (64), linear stability analysis leads to the complete bifurcation diagram in the $\alpha - \beta$ plane, depicted in Figure 1 for two different choices of the diffusion coefficients d, d^u, d^v, corresponding to $\alpha_T > \alpha_{\rm cr}$ (a) and $\alpha_T < \alpha_{\rm cr}$ (b).

More precisely, in Figure 1(a) the steady state $\mathbf{U}^*$ is linearly stable to both homogeneous and nonhomogeneous perturbations at the point $P_1 \equiv (0.8, 0.4)$ lying in the region $\alpha < \alpha_{\rm cr}$. Then, by moving from P_1 to $P_3 \equiv (0.8, 0.59)$, $\mathbf{U}^*$ loses its stability through an Hopf bifurcation occurring at the point $P_2 \equiv (0.8, 0.512)$ so that a time periodic pattern is likely to emerge for $\alpha \in (\alpha_{\rm cr}, \alpha_{\rm ex})$.

On the contrary, Figure 1(b) reveals the occurence of a Turing instability. In fact $\mathbf{U}^*$ is linearly stable at $Q_1 \equiv (0.98, 0.2)$ but it becomes unstable with respect to nonuniform perturbations at $Q_2 \equiv (0.98, 0.3)$ once the Turing bifurcation line $\alpha = \alpha_T$ is crossed.

To complete our analysis we now investigate the inequality (64), which, for fixed values of the cross diffusion coefficients or μ_u^* and ν_v^* respectively, define the $\mu_u^* - \nu_v^*$ or the $d^u - d^v$ stability or Turing regions depending on the values of the kinetic parameters. In detail, in Figure 2 the $\mu_u^* - \nu_v^*$ region is depicted considering three different sets of parameters corresponding to the points P_1, Q_1 (stability region) and Q_2 (Turing region) labelled in Figure 1 whereas in Figure 3 we show the cross-diffusion stability region for fixed values of the constitutive parameters μ_u^*, ν_v^* and kinetic parameters characterizing P_1.

Now, the analytical results obtained hitherto are validated through the numerical integration of the governing system (8) with (57) for $\gamma = \nu^* = 1$ as μ^* is varied. The computation is performed over the spatial domain $[-10, 10]$ by using periodic boundary conditions. More precisely, in Figure 4 we illustrate the dynamics occurring at the point P_1 where $\mathbf{U}^*$ is unconditionally stable so that the system converges to this homogeneous steady state. In Figure 5 dynamics observed at the point P_3 are depicted. Here, according to the linear stability analysis, the numerical results reveal the existence of a limit cycle so that the system moves towards a spatially homogeneous periodic orbit. Moreover, a direct inspection of these figures shows that, in both cases, the system approaches the equilibrium more quickly as the constitutive parameter μ_u^* increases.

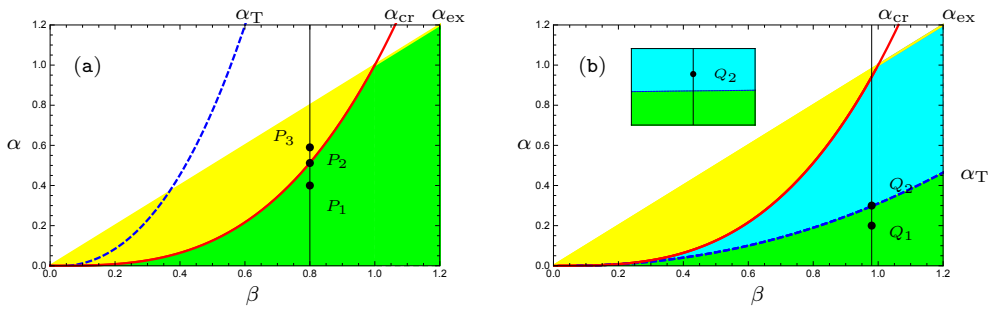

Figure 1: Bifurcation diagram for the steady state $\mathbf{U}^*$ in the $\alpha - \beta$ plane. (a) $d = 0.5$, $d^u = 0.1$, $d^v = 0.08$; (b) $d = 44.98$, $d^u = 1$, $d^v = 1$.

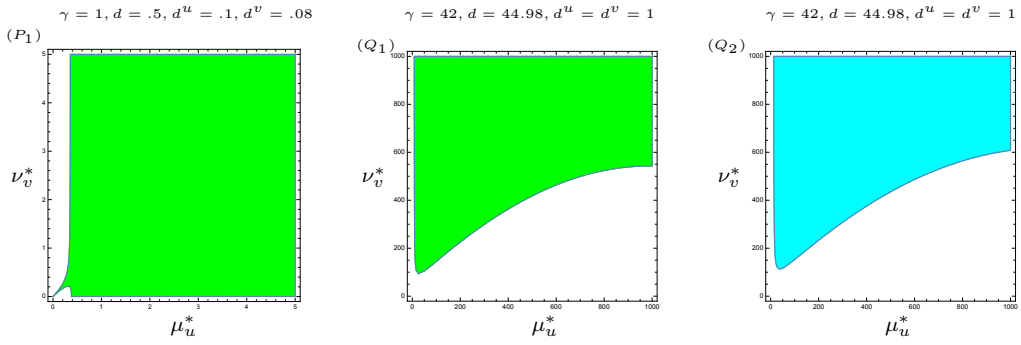

Figure 2: $\mu_u^* - \nu_v^*$ region (coloured) defined by (64) and obtained for fixed values of model parameters corresponding to the representative points P_1, Q_1 and Q_2.

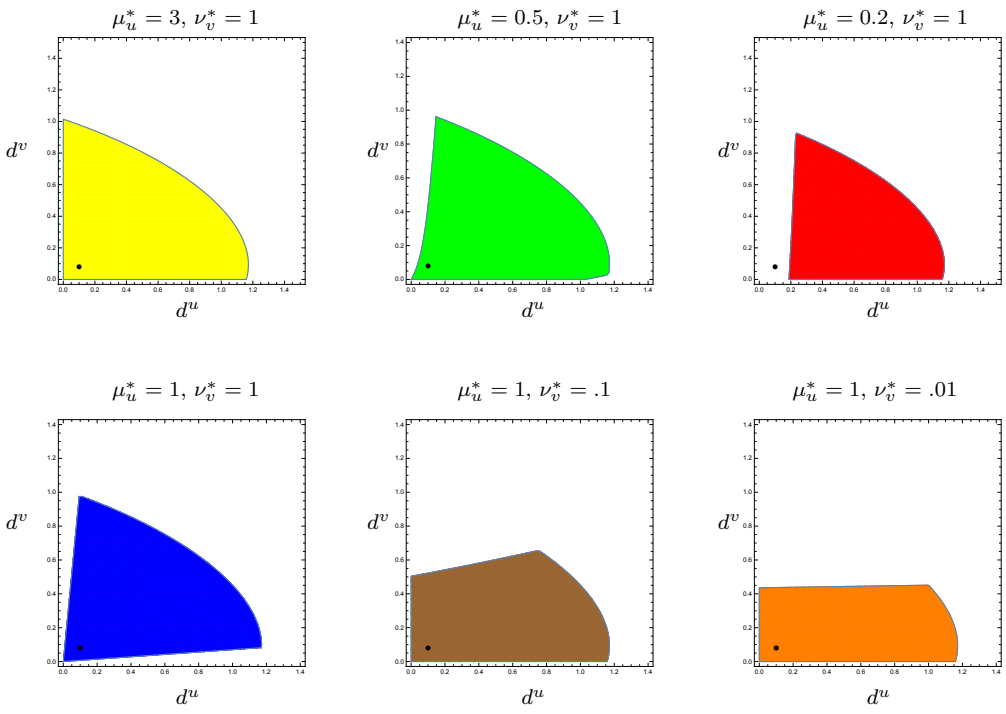

Figure 3: Cross–diffusion stability region (coloured) for $\gamma = 1$, $\alpha = 0.4$, $\beta = 0.8$, $d = 0.5$. The bullet denotes $(.1, .08)$.

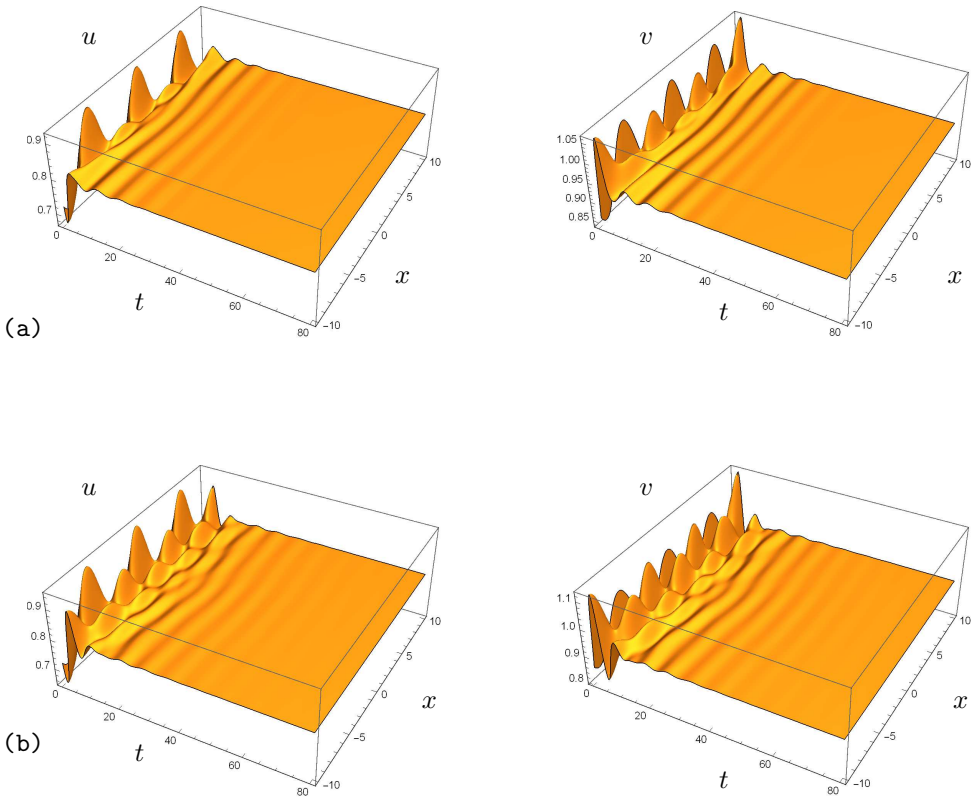

Figure 4: Spatio–temporal evolution of the two chemical species observed at the point P_1 for $\mu_u^* = 3$ (a) and $\mu_u^* = .5$ (b).
The initial data are $u(x,0) = 0.8 + 0.1\cos(x)$, $v(x,0) = 0.9375 + 0.1\cos(x)$, $J^u(x,0) = -0.001$, $J^v(x,0) = -0.01$ with $\gamma = \nu_v^* = 1$.

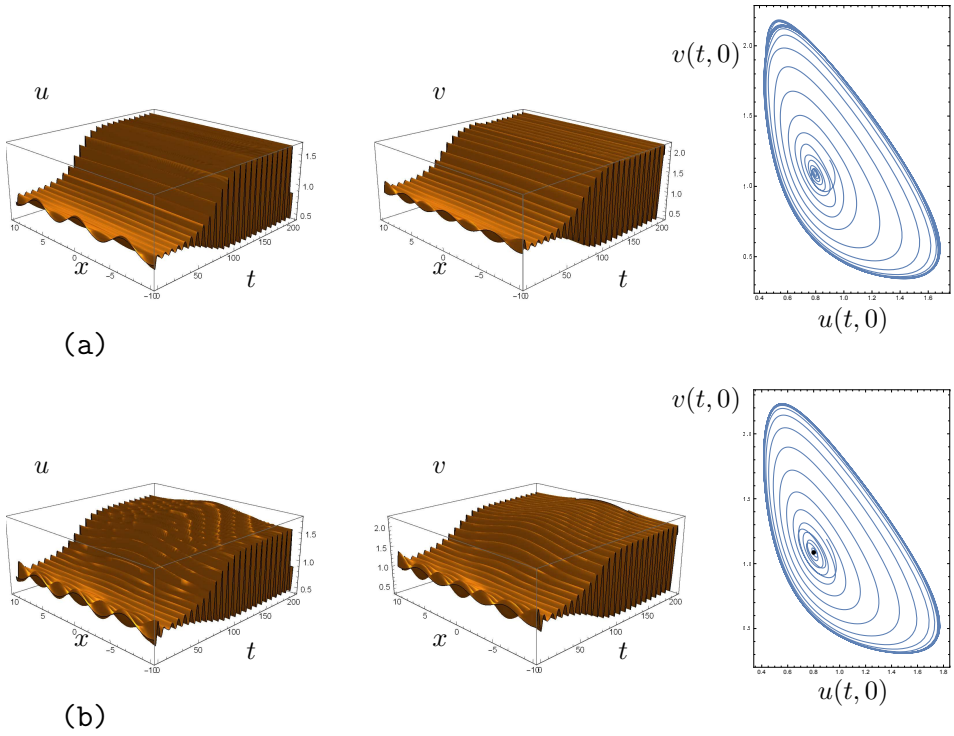

Figure 5: Spatio–temporal evolution of the field variables u and v observed at the point P_3 for $\mu_u^* = 3$ (a) and $\mu_u^* = .5$ (b). The corresponding trajectories in the $u - v$ phase plane are also depicted on the left. The initial data are $u(x,0) = 0.8 + 0.1\cos(x)$, $v(x,0) = 1.08594 + 0.1\cos(x)$, $J^u(x,0) = -0.001$, $J^v(x,0) = -0.01$ with $\gamma = \nu_v^* = 1$.

As far as Turing instability is concerned, the necessary conditions (40) specialize to

$$\begin{aligned} &0 < d^u d^v < d \\ &\alpha_T < \alpha < \min\{\alpha_{\rm cr}, \alpha_{\rm ex}\} \\ &\beta^3 - \alpha d^v > 0 \\ &\xi_2 > 0, \quad \xi_1 + 2\sqrt{\xi_0 \xi_2} > 0 \end{aligned} \tag{67}$$

so that the stationary pattern solution biforcates to the homogeneous steady state at the critical value d_c to which corresponds the critical wave number k_c given by

$$\begin{aligned} d_c &= \frac{\alpha\beta^3(1+d^u)+2\beta^4-\alpha(\alpha+\beta)d^v+2\beta^2\sqrt{(\beta^3-\alpha d^v)(\beta+\alpha(1+d^u))}}{\alpha^2} \\ k_c^2 &= \frac{\gamma\beta}{\sqrt{d_c-d^u d^v}}. \end{aligned} \tag{68}$$

The conditions (67) define a diffusion–driven instability parameter space in which the steady state $\mathbf{U}^*$ is linearly unstable. The hyperbolic character of the model affects these Turing regions via the constitutive parameters μ_u^* and ν_v^* as it is illustrated in Figure 6. More precisely a direct inspection of this figure shows that the instability region may enlarge as the constitutive parameters μ_u^* and ν_v^* grow, i.e. close to the parabolic limit.

Finally, according to the weakly nonlinear analysis developed in Section 4, we deduce the Stuart–Landau equation (49) for the pattern amplitude with

$$\begin{aligned} \sigma &= \frac{d_2 k_c^2\left(\gamma\alpha-\beta k_c^2\right)}{\gamma(\beta^3-\alpha)+\beta(1+d_c)k_c^2+[\gamma k_c^2(\alpha d_c-d^u\beta^3)-\gamma^2\beta^3]\left(\frac{d_c}{\nu_v^*}-\frac{1}{\mu_u^*}\right)} \\ L &= \frac{\beta(p_1+8q_1+4s_1)\left[\gamma+(d^u+1)k_c^2\right]}{8r_2\left\{\gamma(\beta^3-\alpha)+\beta(1+d_c)k_c^2+[\gamma k_c^2(\alpha d_c-d^u\beta^3)-\gamma^2\beta^3]\left(\frac{d_c}{\nu_v^*}-\frac{1}{\mu_u^*}\right)\right\}}. \end{aligned} \tag{69}$$

Let us now accurately investigate the behaviour of the transient regime depending on the sign of the quantity Υ defined in (55). In particular the coefficient of $\left(\frac{d_c}{\nu_v^*}-\frac{1}{\mu_u^*}\right)$ specializes to

$$\frac{\gamma^2\beta\left[(\beta^3-\alpha d^v)(1+\frac{\beta}{\alpha})+\frac{\beta^2}{\alpha}\Delta\right]\left[(\beta^3-\alpha d^v)(1+\frac{\beta}{\alpha})+2\frac{\beta^4}{\alpha}+3\frac{\beta^2}{\alpha}\Delta\right]}{\sqrt{d_c-d^u d^v}\left(\alpha d_c-\beta^3 d^u+\beta^2\sqrt{d_c-d^u d^v}\right)} \tag{70}$$

being

$$\Delta = \sqrt{(\beta^3-\alpha d^v)\left[\beta+(1+d^u)\alpha\right]}. \tag{71}$$

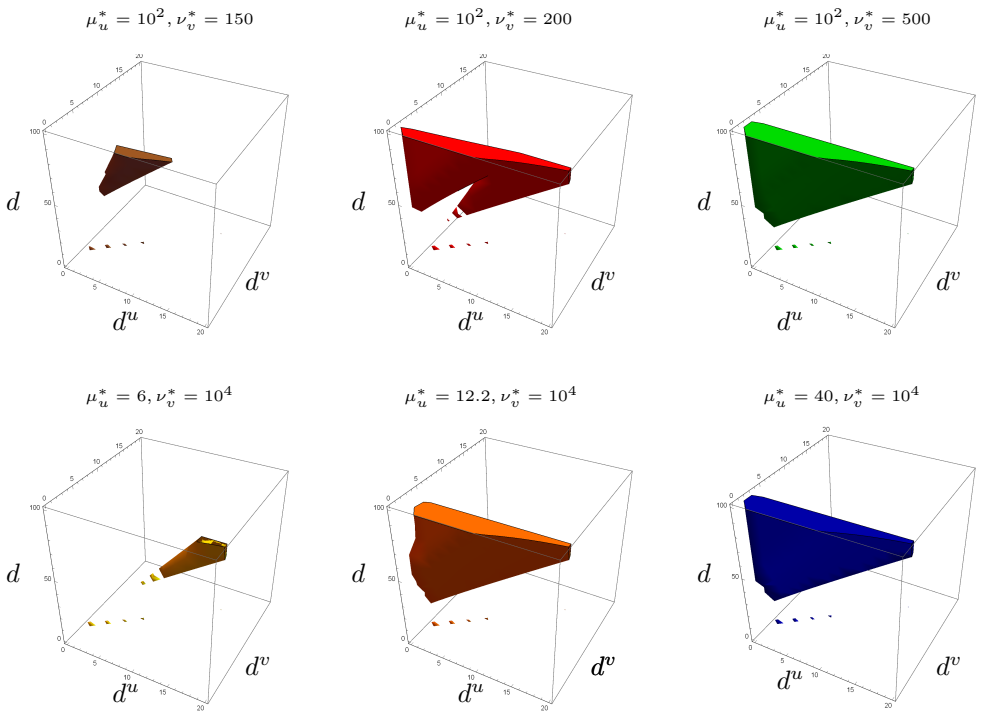

Figure 6: 3D-diffusion Turing region (coloured) for fixed kinetic parameters corresponding to the point Q_2 and obtained as μ_u^* and ν_v^* are varied.

As it is straightforward to ascertain the coefficient (70) is always positive so that the behaviour of the transient regime is completely characterized by the competition between the constitutive parameters μ_u^* and ν_v^*. More precisely, according to the general analysis developed in Section 4, the comparison between the relaxation times evaluated at the threshold, i.e. $\tau^u = \frac{1}{\mu_u^*}$ and $\tau_c^v = \frac{d_c}{\nu_v^*}$, provides relevant informations about the transient times of infinitesimal perturbations. In details, when a small perburbation of the steady state is introduced then the hyperbolic model exhibits exactly the same transient dynamic from $\mathbf{U}^*$ to $\mathbf{U}_\infty$ as that observed in the parabolic limit, even in the presence of "large" relaxation times satysfing condition $\tau^u = \tau_c^v$.

This scenarious is confirmed by the dynamics observed at the point Q_2, lying in the proximity of the Turing biforcation line (see Figure 1(b)), through the numerical solution of the full governing system depicted in Figure 7. Such a numerical investigation has been performed for $\gamma = 42$, $d^u = d^v = 1$ so that $d_c = 43.9864$, $\overline{k}_c = 2.5$, $d = (1+\epsilon^2)d_c$, $\epsilon = 0.12$, by using periodic boundary condition and with the following initial data

$$\begin{aligned} u(x,0) &= 0.98 + 0.001\sin(3x) \\ v(x,0) &= 0.666389 + 0.0001\sin(x) \\ J^u(x,0) &= J^v(x,0) = -10^{-8}. \end{aligned} \tag{72}$$

More precisely, two different sets of phenomenological parameters satisfying the condition $\nu_v^* = \mu_u^* d_c$ have been considered with $\mu_u^* = 14$ (a) and $\mu_u^* = 10^4$ (b). Furthermore Figures 7 (c) confirm that the observed transient dynamic is not affected by the values of the relaxation times.

On the other hand, if $\tau^u < \tau_c^v$, then the system needs a larger time to reach the equilibrium pattern, namely the hyperbolicity enlarges the transient regime as it is predicted by the analytical results obtained in Section 4 (see (56)). From a biological viewpoint it means that when the activator relaxates more quickly than the depletor, then the system needs a longer time to reach the equilibrium pattern. The opposite scenarious appears in the case $\tau^u > \tau_c^v$.

These dynamical behaviours are clearly illustrated in Figure 8 where the spatio–temporal evolution of the Turing patterns exhibited by the hyperbolic model are shown for four different sets of constitutive parameters μ_u^* and ν_v^*. The numerical solution is obtained with the same initial data as well as kinetic parameters values used in Figure 7. These Figures also confirm that the stationary amplitude of the patterns does not depend on the relaxation

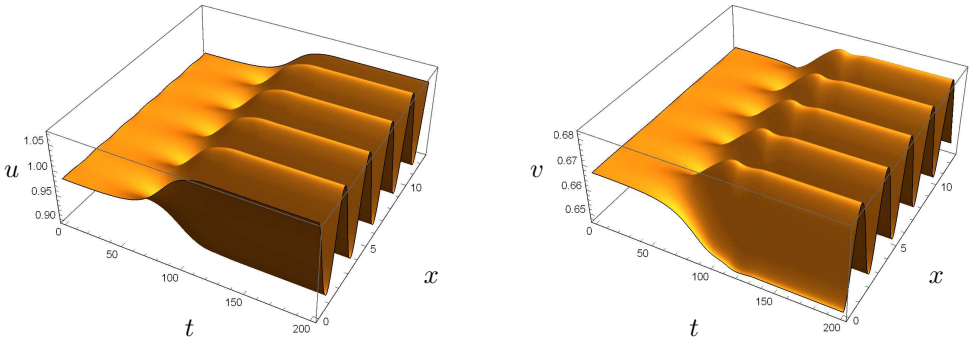

(a) $\tau^u = \tau_c^v = 10^{-4}$

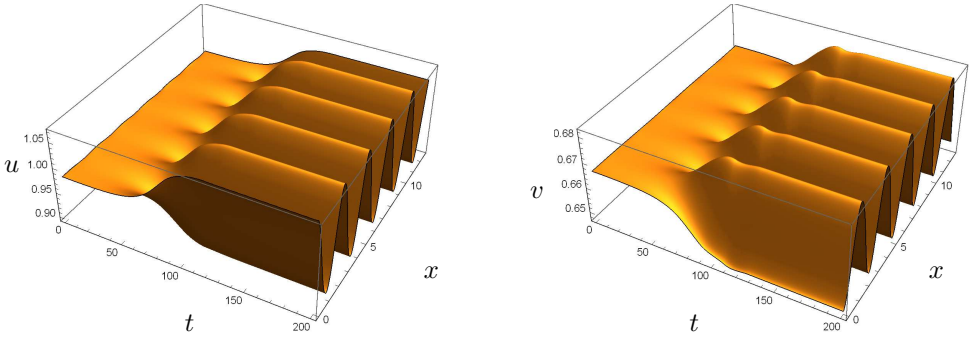

(b) $\tau^u = \tau_c^v = 7 \times 10^{-2}$

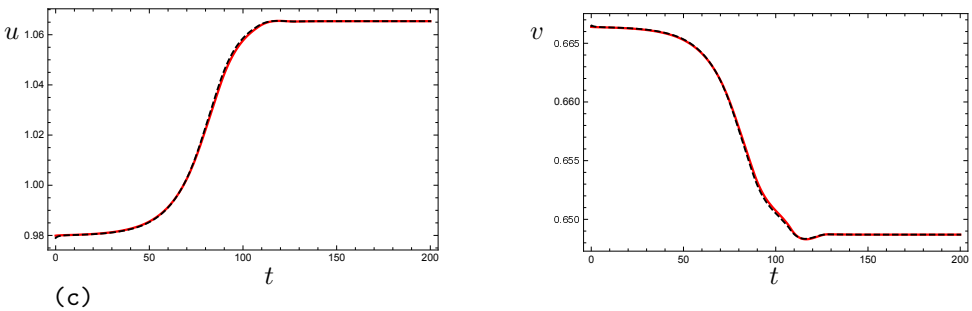

(c)

Figure 7: Numerical solution of the hyperbolic Schnakenberg model with initial data (72) for two set of parameters: $\mu_u^* = 14$, $\nu_v^* = d_c\,\mu_u^*$ (a) and $\mu_u^* = 10^4$, $\nu_v^* = d_c\,\mu_u^*$ (b).
(c) Comparison between the numerical solution represented in (a) (solid line) and (b)(dotted line), evaluated at the illustrative point $x = \frac{5\pi}{2}$.

times and reveal a good agreement between the asymptotic solution (51), predicted by the weakly nonlinear analysis up to $\mathcal{O}(\epsilon^3)$, and the numerical solution.

For the sake of completness the behaviour of the pattern amplitude is reported in Figure 9 for the same parameters set of Figure 7 by considering different values of the phenomenological parameters μ_u^* and ν_v^* .

6 Conclusion

In this paper, following the leading idea of Extended Thermodynamics, we have derived a general class of hyperbolic reaction-diffusion systems modelling those biological phenomena involving both self and cross-diffusion for two interacting species. Then, we have carried out the linear stability analysis of the uniform steady state solutions with respect to both homogeneous and nonhomogeneous perturbations, showing the occurrence of Hopf, Turing and Wave bifurcations. As it is well known, these three kinds of symmetry-breaking bifurcations are responsible for the emergence of patterns which are periodic in time, in space and in both time and space, respectively.

We have investigated the effect of the hyperbolicity on spatial pattern formation pointing out some formal differences between hyperbolic and parabolic models. More precisely, for the class of models at hand, we have observed the occurence of the Wave bifurcation which cannot take place in parabolic two-species reaction-diffusion systems.

For what concerns the Turing bifurcation we have showed that the hyperbolicity does not affect the critical value of the control parameter as well as the unstable modes but the Turing instability region is strongly influenced by the relaxation times.

Then, by performing a weakly nonlinear analysis up to the third order, we have derived the Stuart-Landau equation and deduced the explicit espression of the amplitude of the pattern. As main result, we have been able to pinpoint the mechanism ruling the transient dynamics in the supercritical regime so that interesting differences between parabolic and hyperbolic models have been highlighted. More precisely we have proved that, despite the stationary amplitude of patterns is the same as the one found in the corresponding parabolic model, the manner in which the inhomogeneous steady state is asymptotically reached depends on the relaxation times. Nevertheless, we have also demonstrated that the both parabolic and hyperbolic model ex-

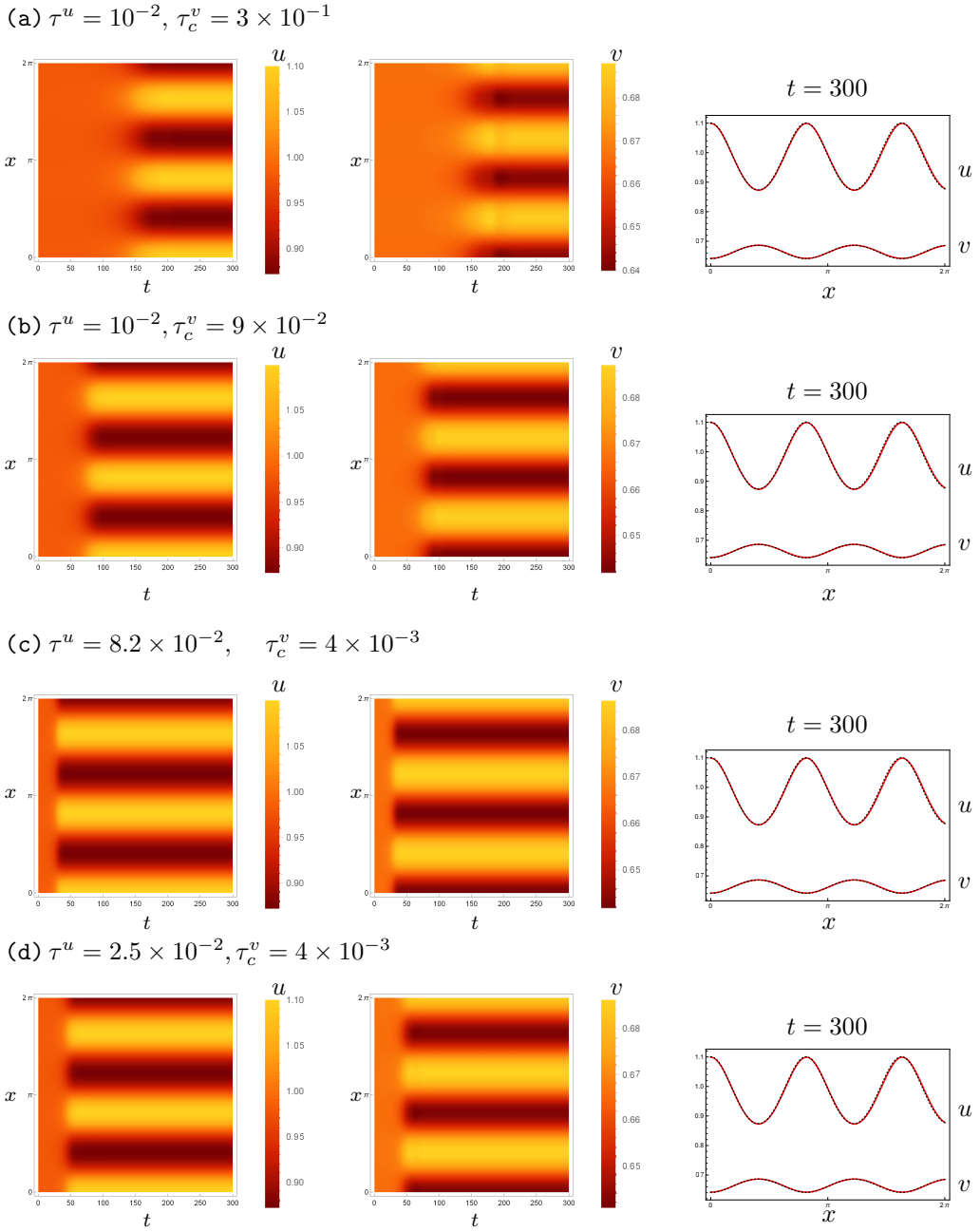

Figure 8: Numerical solution of the hyperbolic Schnakenberg model for $\mu_u^* = 100$ and $\nu_v^* = 150$ (a); $\mu_u^* = 100$ and $\nu_v^* = 500$ (b); $\nu_v^* = 10^4$ and $\mu_u^* = 12.2$ (c); $\nu_v^* = 10^4$ and $\mu_u^* = 40$ (d). The first and the second column show the density plots in the space–time plane of the activator and depletor, respectively, whereas in the third column comparison between the weakly nonlinear solution (dotted line) and the numerical solution (solid line) is depicted.

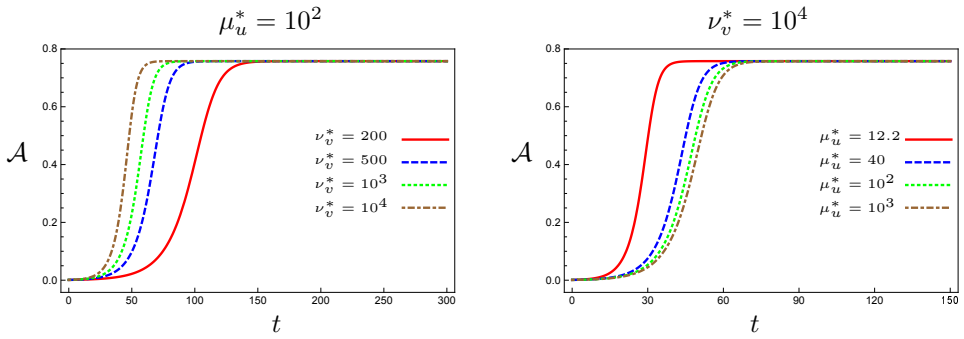

Figure 9: Amplitude pattern evolution obtained for the same parameters as in Figure 7 with initial condition $\mathcal{A}_{in} = 0.001$.

hibits the same transient dynamics not only for very small values of the relaxation times, as expected, but even for large relaxation times when they compensate each other at the excitation threshold. As a consequence, this result predicts the possibility to mimic the whole transient and stationary dynamics observed in the parabolic supercritical regime even in the presence of large relaxation times, i.e. far from the parabolic limit.

Finally, as an illustrative example of the general theory herein developed, we have derived the one-dimensional hyperbolic Schnakenberg model analyzing both linear and weakly nonlinear stability of the uniform steady states. Our theoretical findings are confirmed by several numerical simulations of the governing system.

In this paper we have focused on the supercritical regime, investigations on the subcritical one are actually in progress.

Acknowledgements This work was supported by GNFM–INDAM

References

[1] MC Cross, PC Hohenberg, Pattern formation outside of equilibrium, Reviews of Modern Physics, **65**(3) (1993)851.

[2] R Barreira, CM Elliot, A Madzvamuse, The surface finite element method for pattern formation on evolving biological surfaces, J. Math. Biology, **63**(6)(2011) 1095–1119.

[3] E Barbera, G Consolo, G Valenti, Spread of infectious diseases in a hyperbolic reaction-diffusion susceptible-infected-removed model, Phys. Rev. E, **88** (2013) 052719.

[4] L N Guin, P K Mandal, Spatiotemporal dynamics of reactiondiffusion models of interacting populations, Applied Mathematical Modelling **38** (2014) 4417-4427.

[5] R Cangelosi, JW David, BJ Kealy-Dichone, I Chaiya, Nonlinear stability analyses of Turing patterns for a mussel-algae model, J. Math. Biology, **70**(6) (2015) 1249–1294.

[6] MC Lombardo, R Barresi, E Bilotta, F Gargano, P Pantano, M Sammartino, Demyelination patterns in a mathematical model of multiple sclerosis, J. Math. Biology, **75**(2) (2017) 373–417.

[7] V Vanag, I Epstein,Cross–diffusion and pattern formation in reaction–diffusion system, Phys. Chem. Chem. Phys., **11**(6) (2009) 897–912.

[8] C Tian, Z Lin, M Pedersen, Instability induced by cross–diffusion in reaction–diffusion systems, Nonlinear Anal. Real World Appl., **11**(2)(2010) 1036–1045.

[9] R Ruiz-Baier, C Tian, Mathematical analysis and numerical simulation of pattern formation under cross–diffusion, Nonlinear Anal. Real World Appl. **14**(1) (2013) 601–612.

[10] Z Ling, L Zhang, Z Lin, Turing pattern formation in a predatorprey system with cross diffusion, Applied Mathematical Modelling **38** (2014) 5022–5032.

[11] G Gambino, MC Lombardo, S Lupo, M Sammartino, Super-critical and sub–critical biforcations in a reaction-diffusion Schnakenberg model with linear cross-diffusion,Ricerche di Matematica, **65**(2) (2016) 449–467.

[12] G Gambino, MC Lombardo, M Sammartino, Turing instability and traveling fronts for a nonlinear reaction–diffusion system with cross-diffusion, Mathematics and Computers in Simulation **82** (2012) 1112–1132.

[13] G Gambino, MC Lombardo, M Sammartino, Pattern formation driven by cross–diffusion in a 2D domain, Nonlinear Anal. Real World Appl., **14**(3) (2013) 1755–1779.

[14] A Madzvamuse, HS Ndakwo, R Barreira, Cross–diffusion-driven instability for reaction-diffusion systems: analysis and simulations,J. Math. Biol., **70** (2015) 709–743.

[15] M Banerjee, S Ghorai, N Mukherjee, Study of cross-diffusion induced Turing patterns in a ratio-dependent prey-predator model via amplitude equations, Applied Mathematical Modelling **55** (2018) 383-399.

[16] D Lacitignola, B Bozzini, R Peipmann, I Sgura, Cross-diffusion effects on a morphochemical model for electrodeposition, Applied Mathematical Modelling **57** (2018) 492–513.

[17] EP Zemskov, MA Tsyganov, W Horsthemke, Oscillatory pulse-front waves in a reaction-diffusion system with cross diffusion, Phys. Review E **97** (2018) 062206.

[18] G Gambino, MC Lombardo, M Sammartino, Cross-diffusion-induced subharmonic spatial resonances in a predator-prey system, Physical Review E **97**(2018)012220.

[19] JD Murray, Mathematical Biology II: spatial models and biomedical applications, Springer, 3rd edn., Springer, Berlin 2003.

[20] SR Dunbar, HG Othmer, On a nonlinear hyperbolic equation describing transmission lines, cell movement, and branching random walks. in: HG Othmer (Ed.) Nonlinear Oscillations in Biology and Chemistry, Lecture Notes in Biomathematics, Springer, Berlin, **66** (1986) 274–289.

[21] T Hillen, A Turing model with correlated random walk, J. Math. Biol.,**35** (1996) 49–72.

[22] M AI-Ghoul, B C Eu, Hyperbolic reaction-diffusion equations and irreversible thermodynamics: II. Two-dimensional patterns and dissipation of energy and matter, Physica D **97** (1996) 531–562.

[23] W Horsthemke, Spatial instabilities in reaction random walks with direction-independent kinetics, Phys. Rev. E, **60** (1999). 2651-2666.

[24] KP Hadeler, Reaction Transport Equations in Biological Modeling, Mathematical and Computer Modelling, **31** (2000) 75–81.

[25] J Fort J, V Méndez, Wavefronts in time-delayed reaction-diffusion system. Theory and comparison to experiments. Rep. Prog. Phys., **65**(6) (2002) 895–954.

[26] T Hillen, Hyperbolic models for chemosensitive movement, Math. Models and Methods in Applied Sciences, **12** (2002) 1–28.

[27] V Mendez, S Fedotov, W Horsthemke, Reaction-Transport Systems: Mesoscopic Foundations, Fronts, and Spatial Instabilities, Springer-Verlag Berlin Heidelberg, DOI 10.1007/978-3-642-11443-4 (2010).

[28] R Eftimie, Hyperbolic and kinetic models for self–organized biological aggregations and movement: a brief review, J. Math. Biol., **65** (2012) 35–75.

[29] R Eftimie, G de Vries, MA Lewis, Weakly nonlinear analysis of a hyperbolic model for animal group formation, J. Math. Biol., **59**(1) (2009) 37–74.

[30] E Barbera, C Currò, G Valenti, Wave features of a hyperbolic predator–prey model, Math. Meth. Appl. Sc., **33** (12) (2010) 1504–1515.

[31] B Straughan, Gene–culture shock waves, Phys. Letters A, **377**(88) (2013) 2531–2534.

[32] J Bissel, B Straughan, Discontinuity waves as tipping points: applications to biological and sociological systems, Discrete and Continuous Dynamical Systems-Series B, **19**(7) (2014) 1911–1934.

[33] V Méndez, D Campos, W Horsthemke, Growth and dispersal with inertia: Hyperbolic reaction-transport systems, Physical Review E, **90** (2014) 042114.

[34] E Barbera, C Currò, G Valenti, On discontinuous travelling wave solutions for a class of hyperbolic reaction–diffusion models, Physica D, **308** (2015) 116–126.

[35] PL Buono, R Eftimie, Symmetries and pattern formation in hyperbolic versus parabolic models of self-organised aggregation, J. Math. Biology, **71**(4) (2015) 847–881.

[36] G Consolo, C Curró, G Valenti, Pattern formation and modulation in a hyperbolic vegetation model for semiarid environment, Appl. Math. Modelling, **43** (2017) 372–392.

[37] I Müller, T Ruggeri, Rational Extended Thermodynamics. Springer, New York (1998).

[38] AM Zhabotinsky, M Dolnik, IR Epstein, Pattern formation arising from wave instability in a simple reaction-diffusion system, J. Chem. Phys., **103** (1995) 10306-10314.

[39] L Yang, M Dolnik, AM Zhabotinsky, IR Epstein, Pattern formation arising from interactions between Turing and wave instabilities, J. Chem. Phys., **117** (2002)7259-7265.

[40] RD Parshad, RK Upadhyay, S Mirsha, SK Tiwari, S Sharma, On the explosive instability in a three-species food chain model with modified Holling type IV functional response, Math. Methods Appl. Sciences, **40** (16) (2017) 5707–5726.

[41] IS Liu, Method of Lagrange multipliers for exploitation of the entropy principle, Archive for Rational Mechanics and Analysis, **46** (1972) 131-148.

[42] KO Friedrichs, PD Lax, System of conservation equation with a convex extension, Proceedings of the National Academy of Sciences USA, **61** (1971)1686–1688.

[43] AE Fischer, JE Marsden, The Einstein evolution equations as a first-order quasi-linear symmetric hyperbolic system, I. Commun. Math. Phys., **28** (1972) 1–38.

[44] EP Zemskov, W Horsthemke, Diffusive instabilities in hyperbolic reaction-diffusion equations, Phys. Rev. E, **93**(2016) 032211.

[45] DJ Wollkind, VS Manoranjan, L Zhang, Weakly Nonlinear Stability Analyses of Prototype Reaction-Diffusion Model Equations, SIAM Review, **36**(2) (1994) 176-214.

[46] I Prigogine, R Lefever, Symmetry Breaking Instabilities in Dissipative Systems, J Chem. Phys., **48** (1968) 1695.

[47] A Gierer, H Meinhardt, A theory of biological pattern formation, Kybernetik., **12** (1) (1972) 30–39..

[48] J Schnakenberg, Simple chemical reaction systems with limit cycle behaviour, J Theor Biol., **81** (3) (1979) 389–400.

[49] C Xu, J Wei, Hopf bifurcation analysis in one–dimensional Schankenberg reaction–diffusion model, Nonlinear Anal. Real World Appl., **13** (4) (2012) 1961–1977.

[50] P Liu, J Shi, Y Wang, X Feng, Bifurcation analysis of reaction–diffusion Schankenberg model, J. Math. Chem., **51** (2013)2001–2019.

[51] TW Hwang, HJ Tsai, Uniqueness of the limit cycles in theoretical models of certain oscillating chemical reactions, J. Phys. A, **38** (2005) 8211–8223.

Appendix

In this section we give some details concerning the derivation of the approximate solution (48) as well as of the Stuart–Landau equation (49) obtained by performing the weakly nonlinear analysis.

We consider the set of linear equations (46) for the coefficients $\mathbf{U}_i$ obtained in Section 4

$$\begin{aligned} &\text{at order 1} \quad && \frac{\partial \mathbf{U}_1}{\partial x} - \mathbf{K}^* \mathbf{U}_1 = \mathbf{0} \\ &\text{at order 2} \quad && \frac{\partial \mathbf{U}_2}{\partial x} - \mathbf{K}^* \mathbf{U}_2 = \left(\mathbf{M}^{-1}\right)^* \mathbf{H} \\ &\text{at order 3} \quad && \frac{\partial \mathbf{U}_3}{\partial x} - \mathbf{K}^* \mathbf{U}_3 = \left(\mathbf{M}^{-1}\right)^* \mathbf{N} \end{aligned} \tag{73}$$

with

$$\mathbf{K}^* = \left(\mathbf{M}^{-1} \nabla \mathbf{B}\right)^* \tag{74}$$

$$\mathbf{H} = \frac{1}{2}\left(\left(\mathbf{U}_1 \cdot \nabla_{\mathbf{U}}\right)^{(2)} \mathbf{B}\right)^* - d_1 \left(\frac{\partial \mathbf{M}}{\partial d}\right)^* \frac{\partial \mathbf{U}_1}{\partial x} - \frac{\partial \mathbf{U}_1}{\partial T_1} \tag{75}$$

$$\mathbf{N} = \left[\left(\mathbf{U}_1 \cdot \nabla\right)\left(\left(\mathbf{U}_2 \cdot \nabla\right)\mathbf{B}\right)\right]^* - \left(\frac{\partial \mathbf{M}}{\partial d}\right)^* \left(d_2 \frac{\partial \mathbf{U}_1}{\partial x} + d_1 \frac{\partial \mathbf{U}_2}{\partial x}\right) - \tag{76}$$

$$-\frac{\partial \mathbf{U}_1}{\partial T_2} - \frac{\partial \mathbf{U}_2}{\partial T_1} + \frac{1}{6}\left(\left(\mathbf{U}_1 \cdot \nabla\right)^{(3)} \mathbf{B}\right)^*.$$

As it is usual, $(\mathbf{V}\cdot\nabla)^{(j)}$ denotes the application j times of the operator

$$\mathbf{V}\cdot\nabla = V_1\frac{\partial}{\partial u} + V_2\frac{\partial}{\partial v} + V_3\frac{\partial}{\partial J^u} + V_4\frac{\partial}{\partial J^v}$$

being $\mathbf{V}$ a generic vector.

It is easy to ascertain that the matrix $\mathbf{K}^*$ admits two complex eigenvalues $\pm\,\mathrm{i}\,k_c$ with algebraic and geometric multiplicity given by 2 and 1, respectively. Therefore the general solution of the homogeneous linear system $(46)_1$ is given by

$$\mathbf{U}_1 = \mathbf{P}e^{\mathbf{Q}x}\mathbf{P}^{-1}\mathbf{C}(T_1, T_2, T_3) \tag{77}$$

where $\mathbf{P}$ and $\mathbf{Q}$ denote the invertible transform matrix and the Jordan canonical form of $\mathbf{K}^*$, respectively, that is

$$\mathbf{P} = \begin{bmatrix} \mathrm{i}\,Y_1 & r_1 & -\mathrm{i}\,Y_1 & r_1 \\ \mathrm{i}\,Y_2 & r_2 & -\mathrm{i}\,Y_2 & r_2 \\ Y_3 & \mathrm{i}\,r_3 & Y_3 & -\mathrm{i}\,r_3 \\ Y_4 & \mathrm{i}\,r_4 & Y_4 & -\mathrm{i}\,r_4 \end{bmatrix}, \quad \mathbf{Q} = \begin{bmatrix} \mathrm{i}\,k_c & 0 & 0 & 0 \\ 1 & \mathrm{i}\,k_c & 0 & 0 \\ 0 & 0 & -\mathrm{i}\,k_c & 0 \\ 0 & 0 & 1 & -\mathrm{i}\,k_c \end{bmatrix} \tag{78}$$

with

$$\mathbf{r} = \begin{bmatrix} r_1 \\ r_2 \end{bmatrix}, \quad \widehat{\mathbf{r}} = \begin{bmatrix} -r_3 \\ -r_4 \end{bmatrix}, \quad \mathbf{Y} = \begin{bmatrix} Y_1 \\ Y_2 \end{bmatrix}, \quad \widehat{\mathbf{Y}} = \begin{bmatrix} Y_3 \\ Y_4 \end{bmatrix} \tag{79}$$

satisfying the following systems

$$\begin{aligned} &\left(k_c^2\mathbf{D} - \widetilde{\nabla}\,\mathbf{F}\right)^*\mathbf{r} = 0, \qquad \widehat{\mathbf{r}} = k_c\mathbf{D}^*\mathbf{r} \\ &\left(k_c^2\mathbf{D} - \widetilde{\nabla}\,\mathbf{F}\right)^*\mathbf{Y} = 2\widehat{\mathbf{r}}, \qquad \widehat{\mathbf{Y}} = \mathbf{D}^*\left(k_c\mathbf{Y} - \mathbf{r}\right). \end{aligned} \tag{80}$$

with $\widetilde{\nabla} \equiv \dfrac{\partial}{\partial \mathbf{W}}$.

Hereafter, for the sake of simplicity, we choose $Y_2 = 0$ and, in turn, we obtain

$$Y_1 = \frac{2k_c\left(r_1 + d^v r_2\right)}{\left(k_c^2 - \gamma f_u^*\right)}. \tag{81}$$

Then, by suppressing the secular terms at this order, the solution (77) satisfying zero flux boundary conditions becomes

$$\mathbf{U}_1 = \mathcal{A}(T_1, T_2, T_3)\begin{bmatrix} \mathbf{r}\,\cos\left(k_c\,x\right) \\ \widehat{\mathbf{r}}\,\sin\left(k_c\,x\right) \end{bmatrix} \tag{82}$$

where $\mathcal{A}$ is the amplitude of the pattern which remains undetermined at this stage.

Now, inserting (82) into the nonhomogeous linear system $(46)_2$, the requirement of vanishing secular terms leads to $d_1 = \frac{\partial \mathcal{A}}{\partial T_1} = 0$ so that the solution of $(46)_2$ satisfying zero flux boundary conditions reads

$$\mathbf{U}_2 = \mathcal{A}^2 \left[\begin{array}{c} \mathbf{U}_{20} + \mathbf{U}_{22} \cos(2k_c\, x) \\ \widehat{\mathbf{U}}_{22} \sin(2k_c\, x) \end{array} \right] \tag{83}$$

where $\mathbf{U}_{20}, \mathbf{U}_{22}$ and $\widehat{\mathbf{U}}_{22}$ satisfy

$$\begin{aligned} &\left(\widetilde{\nabla}\mathbf{F}\right)^* \mathbf{U}_{20} = -\frac{1}{2}\left(\mathbf{r}\cdot\widetilde{\nabla}\right)^{(2)}\mathbf{F} \\ &\left(4k_c^2\mathbf{D} - \widetilde{\nabla}\mathbf{F}\right)^* \mathbf{U}_{22} = \frac{1}{2}\left(\mathbf{r}\cdot\widetilde{\nabla}\right)^{(2)}\mathbf{F} \\ &\widehat{\mathbf{U}}_{22} = 2k_c\mathbf{D}^*\mathbf{U}_{22}. \end{aligned} \tag{84}$$

Finally, substituting (82) and (83) into $(46)_3$, the requirement of vanishing resonant terms leads to the following Stuart–Landau equation for the amplitude $\mathcal{A}$

$$\frac{\mathrm{d}\,\mathcal{A}}{\mathrm{d}\,T_2} = \sigma\mathcal{A} - L\,\mathcal{A}^3 \tag{85}$$

where the growth rate σ and the Landau coefficient L are given by

$$\begin{aligned} \sigma &= \frac{d_2 k_c^2\left(\gamma f_u^* - k_c^2\right)}{(1+d_c)k_c^2 - \gamma(f_u^*+g_v^*) + [\gamma k_c^2(d_c f_u^* - d^u f_v^*) - \gamma^2(f_u^* g_v^* - f_v^* g_u^*)]\left(\frac{d_c}{\nu_v^*} - \frac{1}{\mu_u^*}\right)} \\ L &= \frac{(p_1+8q_1+4s_1)\left(k_c^2 d^u - \gamma g_u^*\right) + (p_2+8q_2+4s_2)\left(\gamma f_u^* - k_c^2\right)}{8r_2\left\{(1+d_c)k_c^2 - \gamma(f_u^*+g_v^*) + [\gamma k_c^2(d_c f_u^* - d^u f_v^*) - \gamma^2(f_u^* g_v^* - f_v^* g_u^*)]\left(\frac{d_c}{\nu_v^*} - \frac{1}{\mu_u^*}\right)\right\}} \end{aligned} \tag{86}$$

and the coefficients involved in the expressions of σ and L (86) are given by

$$\begin{aligned} \left[\begin{array}{c} p_1 \\ p_2 \end{array} \right] &= \left(\left(\mathbf{r}\cdot\widetilde{\nabla}\right)^{(3)}\mathbf{F}\right)^*, \\ \left[\begin{array}{c} q_1 \\ q_2 \end{array} \right] &= \left(\mathbf{r}\cdot\widetilde{\nabla}\right)\left(\left(\mathbf{U}_{20}\cdot\widetilde{\nabla}\right)\mathbf{F}\right)^*, \\ \left[\begin{array}{c} s_1 \\ s_2 \end{array} \right] &= \left(\mathbf{r}\cdot\widetilde{\nabla}\right)\left(\left(\mathbf{U}_{22}\cdot\widetilde{\nabla}\right)\mathbf{F}\right)^*. \end{aligned} \tag{87}$$

In particular in the case of the Schnakenberg model the above coefficients specialize to

$$
\begin{aligned}
&p_1 = -p_2 = \tfrac{6\gamma(k_c^2\beta-\alpha\gamma)}{\beta(\beta^2\gamma-k_c^2 d^v)},\\
&q_1 = -q_2 = -\tfrac{(\alpha+\beta)\gamma}{2\beta^3} - \tfrac{2\gamma(k_c^2\beta-\alpha\gamma)}{\beta(\gamma\beta^2-d^v k_c^2)},\\
&s_1 = -s_2 = -\tfrac{q_1}{9\gamma\beta}\left\{2(d^v+d_c)k_c^2\left(\tfrac{\alpha+\beta}{\beta^2} + \tfrac{2(k_c^2\beta-\alpha\gamma)}{\beta^2\gamma-k_c^2 d^v}\right) - \beta\left[\gamma + 4k_c^2(1+d^u)\right]\right\}.
\end{aligned}
\tag{88}
$$